## A new framework for nonlinear Kalman filters $^\star$

Shida Jiang a, Junzhe Shi a, Scott Moura a

<sup>a</sup> Department of Civil and Environmental Engineering, University of California, Berkeley, CA, USA

#### Abstract

The Kalman filter (KF) is a state estimation algorithm that optimally combines system knowledge and measurements to minimize the mean squared error of the estimated states. While KF was initially designed for linear systems, numerous extensions of it, such as extended Kalman filter (EKF), unscented Kalman filter (UKF), cubature Kalman filter (CKF), etc., have been proposed for nonlinear systems over the last sixty years. Although different types of nonlinear KFs have different pros and cons, they all use the same framework of linear KF. Yet, according to our theoretical and empirical analysis, the framework tends to give overconfident and less accurate state estimations when the measurement functions are nonlinear. Therefore, in this study, we designed a new framework that can be combined with any existing type of nonlinear KFs and showed theoretically and empirically that the new framework estimates the states and covariance more accurately than the old one. The new framework was tested on four different nonlinear KFs and five different tasks, showcasing its ability to reduce estimation errors by several orders of magnitude in low-measurement-noise conditions. The codes are available at https://github.com/Shida-Jiang/A-new-framework-for-nonlinear-Kalman-filters

Key words: Kalman filtering; nonlinear observer and filter design; extended Kalman filter; unscented Kalman filter; estimation theory; parameter and state estimation

## 1 Introduction

In control theory, the Kalman filter (KF) is a state estimation algorithm designed for linear systems. In such a system, a set of linear state transition functions describes how the states evolve, and a set of linear measurement functions describes the measured values of certain linear combinations of states. It is assumed that both the state transition and measurement functions contain some additive noise. Among all linear estimators, the KF optimally combines the system knowledge and measurements to minimize the expected value of the meansquared error of the state estimation. Additionally, when the process noise, measurement noise, and state estimation errors all follow a multivariate normal (Gaussian) distribution, the state estimation given by the Kalman filter is also the maximum likelihood estimation [1]. Due to these desirable features, KF is often referred to as the optimal linear state estimator. Since its birth in about 1960, KF has achieved massive success in navigation [2], motion control [3], statistics [4], signal processing [5], etc.

Email addresses: shida\_jiang@berkeley.edu (Shida Jiang), junzhe\_shi@berkeley.edu (Junzhe Shi), smoura@berkeley.edu (Scott Moura).

The most significant limitation of KF is that it can only be applied to systems with linear state transition functions and linear measurement functions. Unfortunately, many real-life systems are nonlinear [6]. Therefore, some extensions of KF have been developed to solve the state estimation problem for these nonlinear systems, and the most well-known ones are the extended Kalman filter (EKF) and the unscented Kalman filter (UKF).

EKF linearizes the state transition functions and measurement functions locally at each time step [6]. This technique transforms the nonlinear system into a linear system, where KF can be directly applied. While EKF is relatively simple, the linearization performed in each step neglects the higher-order derivatives, making the state estimations biased and overconfident. Specifically, estimations can be biased since  $\mathbb{E}(f(x)) = f(\mathbb{E}(x))$  is not guaranteed for a nonlinear function, and overconfidence arises when the actual variance is much higher than estimated. These problems are partially solved by the second-order extended Kalman filter (EKF2) [7], which approximates the nonlinear system by its second-order Taylor expansion. However, EKF2 requires the calculation of the Hessian matrix of each state transition function and measurement function, which adds non-trivial computational complexity to the algorithm. Additionally, EKF2 still sometimes gives inaccurate and overcon-

 $<sup>^\</sup>star$  This paper was not presented at any IFAC meeting. Corresponding author Shida Jiang Tel. +1 510-944-9339.

fident estimations, so it is generally used less frequently than EKF.

Classical EKF and EKF2 formulations are usually presented in a way that requires explicit Jacobian matrices of the state-transition and measurement functions, which may not always be accessible or convenient to compute in real-world systems. Although derivative-free variants of the EKF and EKF2 have been proposed [8,9]. a particularly influential derivative-free extension of the KF to nonlinear systems is the UKF. In 1997, Julier and Uhlmann introduced a derivative-free extension of the KF to nonlinear systems that avoids explicit Jacobian computations and mitigates the accuracy loss caused by first-order linearization [10]. In later literature, this extension is usually referred to as the UKF [11]. The UKF approximates the mean and covariance of the states after nonlinear transformations by propagating a set of deterministically chosen sigma points around the estimated state mean. These sigma points are constructed from the square root of the state covariance matrix so that their weighted mean and covariance match the prior mean and covariance. After applying the nonlinear transformation to each sigma point, the transformed mean and covariance are recovered as weighted averages of the transformed points, which typically yields a more accurate approximation of the first two moments than a firstorder linearization. Similar ideas have also been used in several other nonlinear KFs, including cubature Kalman filter (CKF) [12], quadrature Kalman filter [13], squareroot quadrature Kalman filter [14], etc. All these filters use deterministic ways to find several additional points around the central point (the estimated states from the previous iteration) and use those points to approximate the first two moments of the states after the nonlinear transformation. All these methods have some links with EKF2. As pointed out by Gustafsson et al. in [9], when the sigma points are infinitely close to the center, and the hyperparameters in the UKF are set to specific values, UKF will give the same state estimation as the EKF2, although the covariance estimation can still be a bit different. A disadvantage of these nonlinear KFs is that the number of sampling points is usually twice the number of states. Therefore, the method can be increasingly more complicated than EKF as the number of states increases.

While different extensions of the Kalman filter (KF) approximate the first- and second-order moments of the state after a nonlinear transformation in different ways, they all retain the same algorithmic structure as the linear KF. In this paper, we refer to this structure as the "conventional framework" or "old framework". In each iteration, the estimation process consists of two stages: Predict and Update. In the "predict" step, the state mean and covariance are propagated through the process model using the estimates from the previous iteration. In the "update" step, the incoming measurement is used to correct the state prediction through a feedback

term known as the Kalman gain. In the linear KF, this gain is analytically derived to minimize the trace of the a posteriori covariance matrix, and the corresponding covariance is then updated consistently with this optimal gain.

While this framework is the optimal linear state estimator for linear systems, applying it to nonlinear measurement functions often results in overconfident covariance estimates and degraded state accuracy. The fundamental issue is that the Kalman gain is computed as though it still minimizes the posterior covariance trace, even though this optimality no longer holds when the required moments are only approximated. As we will show later, the "update" step may even increase the estimation error in nonlinear systems. Consequently, the implicit assumption of optimality in the "update" step can be very harmful, because the filter becomes increasingly confident in estimates that are systematically biased or inaccurate.

The overconfidence phenomenon described above is well known in the literature. Graphical illustrations of EKF overconfidence have been provided in [15], and in the context of simultaneous localization and mapping (SLAM), researchers have repeatedly observed that nonlinear KFs tend to produce overconfident, rather than conservative, state estimates, especially after a long time [16–18]. Moreover, this overconfidence issue becomes more pronounced when the measurement noise variance is small [19, 20], because the linearization (or other approximation) error then constitutes a larger fraction of the total error budget, making the filter's covariance underestimate more severe. In some cases, this leads to a highly undesirable and counterintuitive behavior: the actual estimation error increases as the measurement noise decreases. The underlying reason is that the actual estimation errors decrease much more slowly than the estimated standard deviations, so the filter becomes overconfident and is less able to correct itself in later iterations. As sensor technology continues to improve and measurement noise is further reduced across many applications, we can reasonably expect this problem to become even more severe if we continue to rely on the conventional framework for nonlinear KFs.

Unfortunately, so far, there is no general solution that can effectively prevent the nonlinear KF from overconfidence and improve its estimation accuracy. Although it is possible to mitigate the problem by approximating the measurement function at higher orders (e.g., using EKF2 instead of EKF), these algorithms take a significantly longer computational time, and the problem will still, in general, exist. The lack of theoretical analysis for nonlinear KFs makes finding a general solution even harder. For those few existing theoretical analyses [9, 19, 21], the results are based on the assumption that the higher-ordered terms in the Taylor expansions of the measurement functions can be ignored. This as-

sumption may not be reasonable because the predicted states can be very far away from the updated states, and ignoring higher-ordered terms can cause significant errors in the "update" step.

Apart from modifying the structure of the filter itself, another widely used strategy for mitigating filter overconfidence is covariance inflation [22,23]. In this approach, the estimated state covariance is deliberately enlarged, and the associated inflation factor is adjusted to compensate for under-dispersion and errors caused by nonlinearity. While covariance inflation can alleviate overconfidence, its performance depends heavily on the choice of the inflation factor, whose value typically requires extensive fine-tuning. This tuning can be computationally costly and problem-dependent, thereby undermining the universality of the approach [24, 25].

In this study, we propose a new framework that solves the problem of overconfidence. The key idea of the new framework is to add a step that reevaluates the actual effect of the Kalman gain after the state update. With this additional step, the state covariance estimation can be much more accurate, and any unhelpful update can be withdrawn. The main contributions of this paper are:

- To the best of our knowledge, we are the first to give a mathematical proof that the conventional framework for nonlinear KFs, which has been used for around sixty years, generally has the problem of underestimating the trace of the state covariance matrix.
- We proposed a new framework to solve the problem of inaccurate covariance estimation and validated the framework's effectiveness by using both theoretical and empirical analysis.
- The proposed new framework can be combined with almost any type of nonlinear KF and reduce the state estimation error by more than an order of magnitude in various applications when the measurement noise is low.

The rest of the paper is organized as follows. Section 2 conducts a rigorous theoretical analysis of the problem of the conventional framework for nonlinear KFs and introduces a new framework that solves the problem. Section 3 presents a comprehensive comparison between the two frameworks. Specifically, both frameworks are combined with four different types of nonlinear KFs and validated on five distinct applications. The conclusions are drawn in Section 4.

## 2 Method

#### 2.1 General formulation of nonlinear Kalman filters

Consider a discrete-time system with nonlinear dynamics

$$x_k = f(x_{k-1}, u_{k-1}) + w_{k-1}, \tag{1}$$

where  $x_k$  denotes the (unknown) true states at time step k,  $u_{k-1}$  is the known input applied between time steps k-1 and k, and  $w_{k-1}$  is the process noise, assumed zeromean with covariance  $Q_{k-1}$ , and independent of  $x_{k-1}$  and past measurements. At time step k-1, the filter maintains an a posteriori state estimate  $\hat{x}_{k-1|k-1}$  with associated error covariance  $P_{k-1|k-1}$ .

For any nonlinear KF variant, the first step of each iteration is the "predict" step, which propagates  $\hat{x}_{k-1|k-1}$  and  $P_{k-1|k-1}$  through the process model (1) to obtain the a priori quantities  $\hat{x}_{k|k-1}$  and  $P_{k|k-1}$ . The predicted state estimate at time step k is denoted by  $\hat{x}_{k|k-1}$ , and the corresponding estimation error  $x_k - \hat{x}_{k|k-1}$  is assumed to follow a zero-mean multivariate distribution with covariance  $P_{k|k-1}$ . Formally,

$$\begin{cases}
\mathbb{E}[x_k - \hat{x}_{k|k-1}|z_{1:k-1}] = 0, \\
P_{k|k-1} = \operatorname{Var}(x_k - \hat{x}_{k|k-1}|z_{1:k-1}),
\end{cases}$$
(2)

where  $z_{1:k-1}$  denotes the past measurements. In the subsequent analysis, we work conditionally on the observation history. In particular, for any fixed realization of  $z_{1:k-1}$ ,  $P_{k|k-1}$  is a deterministic function of that realization; likewise,  $P_{k-1|k-1}$  is deterministic given  $z_{1:k-1}$ . Unless stated otherwise, we suppress the conditioning in the notation for all means, covariances, and crosscovariances (e.g.,  $P_{k|k-1}$ ,  $P_{z,k}$ ,  $P_{xz,k}$ , and  $S_k$ , which will be formally defined later).

The second step of each iteration for a nonlinear KF is called the "update", which corrects the predicted state based on the new measurement. The measurement model is

$$z_k = h(x_k) + v_k, (3)$$

where  $z_k$  is the measurement at time step k, and  $v_k$  is the measurement noise, assumed zero-mean with covariance  $R_k$ . Given the predicted state, the measurement can be predicted (using a specific nonlinear KF algorithm), and we denote this predicted measurement by  $\hat{z}_{k|k-1}$ . The corresponding (noise-free) prediction error  $h(x_k) - \hat{z}_{k|k-1}$  is assumed zero-mean with covariance  $P_{z,k}$ . The cross-covariance between the state prediction error and the measurement prediction error is denoted by  $P_{xz,k}$ .

The difference between the actual and predicted measurements is called the measurement residual (or innovation), denoted by

$$\tilde{z}_k := z_k - \hat{z}_{k|k-1}. \tag{4}$$

Since both  $v_k$  and  $h(x_k) - \hat{z}_{k|k-1}$  are zero-mean, the innovation  $\tilde{z}_k$  is also zero-mean. If, in addition, the measurement noise  $v_k$  is assumed to be independent of the (noise-free) prediction error  $h(x_k) - \hat{z}_{k|k-1}$ , the covari-

ance of the innovation is

$$S_k = P_{z,k} + R_k. (5)$$

The KF update for the state estimate is

$$\hat{x}_{k|k} = \hat{x}_{k|k-1} + K_k \tilde{z}_k, \tag{6}$$

where  $\hat{x}_{k|k}$  is the updated state estimate and  $K_k$  is the Kalman gain at time step k. Using (4)–(6), the a posteriori error covariance can be written as [26]

$$P_{k|k} = P_{k|k-1} + K_k S_k K_k^T - P_{xz,k} K_k^T - K_k P_{xz,k}^T.$$
 (7)

The Kalman gain  $K_k$  is chosen to minimize  $\operatorname{tr}(P_{k|k})$ . By differentiating  $\operatorname{tr}(P_{k|k})$  in (7) with respect to  $K_k$ , we obtain the optimal gain

$$K_{k,\text{op}} = P_{xz,k} S_k^{-1},\tag{8}$$

where  $K_{k,\text{op}}$  denotes the optimal Kalman gain. Substituting (8) into (7) yields the well-known expression

$$P_{k|k,\text{op}} = P_{k|k-1} - K_{k,\text{op}} S_k K_{k,\text{op}}^T.$$
 (9)

Equations (6)–(9) summarize the key principle of KF: the state estimate is updated in such a way that the trace of the a posteriori error covariance is minimized. However, for systems with nonlinear measurement functions  $h(\cdot)$ , these expressions involve covariance terms  $P_{k|k-1}$ ,  $P_{z,k}$ ,  $S_k$ , and  $P_{xz,k}$  that, in general, are defined as expectations with respect to the full distribution of the state and cannot be uniquely determined from the first two moments alone. Since nonlinear KFs propagate only the mean and covariance of the state, this information is generally insufficient to recover the true values of these matrices, so they must be approximated. In fact, as we will show next, inaccurate approximations regarding these matrices are the key factors that can make the conventional framework for nonlinear KFs overconfident and inaccurate.

Before concluding this subsection, we note that the formulation above extends directly to non-additive noise. Specifically, if the process noise enters the dynamics as  $x_k = f(x_{k-1}, u_{k-1}, w_{k-1})$ , we can define the prediction-time augmented variable  $\chi_{k-1} := [x_{k-1}^T \ w_{k-1}^T]^T$ . Likewise, if the measurement noise is non-additive,  $z_k = h(x_k, v_k)$ , we can define the update-time augmented variable  $\eta_k := [x_k^T \ v_k^T]^T$ . Since the first two moments of these augmented variables are determined by the first two moments of  $x_{k-1}, w_{k-1}$ , and  $v_k$ , the same algorithmic machinery (e.g., linearization or sigma-point propagation) applies to  $\chi_{k-1}$  and  $\eta_k$  to approximate the first two moments of  $x_k$  and  $z_k$ . Importantly,  $w_{k-1}$  and  $v_k$  are not treated as persistent states; they are i.i.d. zero-mean draws at each step and are included in the augmentation only to capture their nonlinear effect on the moments.

2.2 The conventional framework and its problem

While calculating the actual values of  $P_{k|k-1}$ ,  $P_{z,k}$ ,  $S_k$ , and  $P_{xz,k}$  is generally impossible by just using the first two moments of the states, it is possible to make some approximations. Without loss of generality, this problem of approximation can be formulated as follows.

The general approximation problem in nonlinear Kalman filters: Given an estimated mean  $\hat{X} \approx \mathbb{E}[X]$  and an estimated covariance  $P_{x,\text{est}} \approx \text{Var}(X)$  of the state X, and a nonlinear mapping Y = g(X), we seek to approximate  $\mathbb{E}[Y]$ , Var(Y), and Cov(X,Y). The solution can be generally written as

$$\begin{cases} \hat{Y} := \Phi_{e}(g; \hat{X}, P_{x, \text{est}}) \approx \mathbb{E}[Y], \\ P_{y, \text{est}} := \Phi_{y}(g; \hat{X}, P_{x, \text{est}}) \approx \text{Var}(Y), \\ P_{xy, \text{est}} := \Phi_{xy}(g; \hat{X}, P_{x, \text{est}}) \approx \text{Cov}(X, Y), \end{cases}$$
(10)

where  $\Phi_e$ ,  $\Phi_y$ , and  $\Phi_{xy}$  denote the approximation mappings determined by the chosen nonlinear KF (e.g., EKF, UKF, CKF). The nonlinear mapping g may represent either the state transition function f (prediction step) or the measurement function h (update step), so this approximation problem is typically solved at least twice in each iteration of a nonlinear KF. Specifically,  $P_{k|k-1}, P_{z,k}, S_k$ , and  $P_{xz,k}$  can be respectively approximated by:

$$\begin{cases}
P_{k|k-1,\text{est}} := \Phi_{y}(f; \hat{x}_{k-1|k-1}, P_{k-1|k-1,\text{est}}) + Q_{k-1}, \\
P_{z,k|k-1} := \Phi_{y}(h; \hat{x}_{k|k-1}, P_{k|k-1,\text{est}}), \\
S_{k|k-1} := P_{z,k|k-1} + R_{k}, \\
P_{xz,k|k-1} := \Phi_{xy}(h; \hat{x}_{k|k-1}, P_{k|k-1,\text{est}}).
\end{cases} (11)$$

Note that the subscript k|k-1 means that the covariance matrices are all estimated based on the predicted states  $\hat{x}_{k|k-1}$ .

Although the corresponding  $\Phi_y$ ,  $\Phi_s$ , and  $\Phi_{xy}$  differ, all existing types of nonlinear KFs directly replace  $P_{k|k-1}$ ,  $S_k$ , and  $P_{xz,k}$  in (8) and (9) with the approximated values in (11). Namely, the Kalman gain is selected as

$$K_{k,\text{est}} := P_{xz,k|k-1} S_{k|k-1}^{-1},$$
 (12)

and the state covariance matrix is updated by

$$P_{k|k,\text{est}} := P_{k|k-1,\text{est}} - K_{k,\text{est}} S_{k|k-1} K_{k,\text{est}}^T$$

$$= P_{k|k-1,\text{est}} - P_{xz,k|k-1} S_{k|k-1}^{-1} P_{xz,k|k-1}^T.$$
(13)

On the other hand, the actual value of the updated state covariance matrix  $P_{k|k,ac}$  given the selected Kalman gain in (12) can be calculated by substituting (12) into (7).

Namely,

$$P_{k|k,ac} = P_{k|k-1} + P_{xz,k|k-1} S_{k|k-1}^{-1} S_k S_{k|k-1}^{-1} P_{xz,k|k-1}^T - P_{xz,k} S_{k|k-1}^{-1} P_{xz,k|k-1}^T - P_{xz,k|k-1} S_{k|k-1}^{-1} P_{xz,k}^{-1}.$$
(14)

The covariance estimation error after the state update can therefore be calculated as

$$P_{k|k,\text{err}} := P_{k|k,\text{ac}} - P_{k|k,\text{est}}.$$
 (15)

Noticing that the covariance estimation error before the state update is

$$P_{k|k-1,\text{err}} := P_{k|k-1} - P_{k|k-1,\text{est}}, \tag{16}$$

the change in the covariance estimation error is

$$\Delta P_{k|k,\text{err}} := P_{k|k,\text{err}} - P_{k|k-1,\text{err}} 
= P_{k|k,\text{ac}} - P_{k|k,\text{est}}|_{P_{k|k-1,\text{est}} = P_{k|k-1}}.$$
(17)

 $\Delta P_{k|k,\text{err}}$  defined in (17) represents the magnitude of overconfidence brought by the state update. When  $\Delta P_{k|k,\text{err}}$  is positive semi-definite, it means that the estimate becomes more overconfident after the state update, and vice versa. Note that  $P_{k|k,ac}$  plays the role of  $P_{k|k}$  in (7), and  $P_{k|k,\text{est}}$  plays the role of  $P_{k|k,\text{op}}$ in (9). Intuitively,  $\operatorname{tr}(P_{k|k,ac})$  tends to be larger than  $\operatorname{tr}(P_{k|k,\mathrm{est}})$  since  $\operatorname{tr}(P_{k|k,\mathrm{op}}) = \min \operatorname{tr}(P_{k|k}) \le \operatorname{tr}(P_{k|k})$ . However, this relationship of size is not always preserved after the approximations. For example, according to (13) and (14), when  $P_{xz,k} = S_k = 1$  and  $P_{xz,k|k-1} = S_{k|k-1} = 0.9$ , we have  $\Delta P_{k|k,\text{err}} = 0.1 > 0$ . Nevertheless, in most cases in practice [27, 28], we do find that  $\operatorname{tr}(P_{k|k,ac}) > \operatorname{tr}(P_{k|k,est})$ , meaning that using (13) will often (although not always) underestimate the actual covariance.

To formalize this idea, we interpret the approximated covariance matrices  $P_{z,k|k-1}$ ,  $S_{k|k-1}$ , and  $P_{xz,k|k-1}$  produced by a nonlinear KF as (random) estimators of the actual quantities  $P_{z,k}$ ,  $S_k$ , and  $P_{xz,k}$ . More precisely, we regard  $P_{xz,k|k-1}$  as a random matrix,  $P_{z,k|k-1}$  as a random positive semidefinite matrix, and  $S_{k|k-1}$  as a random positive definite matrix. For clarity, all such random covariance matrices are marked in red in this section. Additionally, we assume that these approximated covariance matrices are unbiased estimators and satisfy

$$\begin{cases}
\mathbb{E}[P_{z,k|k-1}] = P_{z,k}, \\
\mathbb{E}[S_{k|k-1}] = S_k, \\
\mathbb{E}[P_{xz,k|k-1}] = P_{xz,k}.
\end{cases}$$
(18)

These additional definitions and assumptions are introduced to facilitate consideration of the "average" case

and provide a more mathematically rigorous definition of the overconfidence caused by (13). Specifically, (18) should be understood as follows. If a systematic, nonzero-mean bias in these approximations were known a priori, it would be natural to modify the filter so as to subtract this bias, and to analyze only the residual approximation error. Thus, it is reasonable to model the remaining covariance errors as zero-mean random matrices. Note that this viewpoint is conceptually analogous to the standard treatment of deterministic biases in augmented-state or separate-bias Kalman filters, where unknown biases are initialized as zero-mean random variables. Namely, any known mean component is absorbed into the system model, and only the zero-mean uncertainty is left for the filter to estimate.

With (18), we have the following theorem about the overconfidence of nonlinear Kalman filters.

**Theorem 1** Suppose that  $P_{xz,k|k-1}$  and  $S_{k|k-1}$  are random matrices that satisfy (18).  $S_{k|k-1}$  is symmetric and positive definite. Then,  $\Delta P_{k|k,\text{err}}$  calculated from (17) satisfies:

$$\mathbb{E}[\Delta P_{k|k,\text{err}}] \succeq 0, \tag{19}$$

where " $\succeq$ " represents positive semidefiniteness, and the equality only holds when  $P_{xz,k|k-1}S_{k|k-1}^{-1}$  is constant almost surely. Note that this theorem does not require  $P_{xz,k|k-1}$  and  $S_{k|k-1}$  to be independent.

**PROOF.** Let  $P = P_{xz,k|k-1}S_k^{-\frac{1}{2}}$ ,  $S = S_k^{-\frac{1}{2}}S_{k|k-1}S_k^{-\frac{1}{2}}$ . According to (18),

$$\begin{cases} \mathbb{E}[\mathbf{P}] = \bar{P} = P_{xz,k} S_k^{-\frac{1}{2}}, \\ \mathbb{E}[\mathbf{S}] = I. \end{cases}$$
 (20)

According to (13, 14, 18),

$$\Delta P_{k|k,\text{err}} = PS^{-2}P^T - \bar{P}S^{-1}P^T - PS^{-1}\bar{P}^T + PS^{-1}P^T 
= (PS^{-1} - \bar{P})(PS^{-1} - \bar{P})^T + PS^{-1}P^T - \bar{P}\bar{P}^T.$$
(21)

For any fixed unit vector v,  $P^T v$  is a random vector with a mean of  $\bar{P}^T v$ . According to Lemma 4 in Appendix A,

$$\mathbb{E}[\boldsymbol{v}^T \boldsymbol{P} \boldsymbol{S}^{-1} \boldsymbol{P}^T \boldsymbol{v}] \ge \boldsymbol{v}^T \bar{P} \bar{P}^T \boldsymbol{v}. \tag{22}$$

Moving the right hand side to the left, we get

$$\mathbb{E}[PS^{-1}P^T - \bar{P}\bar{P}^T] \succeq 0. \tag{23}$$

Therefore, the expectation of (21) is always positive semi-definite. due to (23) and the fact that the first term in (21) is positive semi-definite. The equality only holds when  $PS^{-1}$  is constant almost surely, which is equivalent to  $K_{k,\mathrm{est}} = P_{xz,k|k-1}S_{k|k-1}^{-1}$  being constant (i.e., free from approximation errors) almost surely.

Theorem 1 suggests that using (13) to estimate the state covariance matrix tends to lead to overconfident covariance estimation when the estimated  $S_k$  and  $P_{xz,k}$  are not the same as their actual values. Admittedly, in practice, the errors of the approximated covariance matrices  $P_{z,k|k-1}$ ,  $S_{k|k-1}$ , and  $P_{xz,k|k-1}$  may not be as simple as zero-mean random matrices. However, Theorem 1 does give us a structured explanation as to why nonlinear KFs often underestimate the state covariance matrix. Note that an overconfident state covariance estimation can be very detrimental since it prevents the filter from correcting itself in subsequent iterations, thereby affecting the state estimation accuracy. Again, this problem is unavoidable because the actual values of  $S_k$  and  $P_{xz,k}$ are related to the actual distribution of the states, which is unknown. Therefore, this problem exists for all types of nonlinear KFs as long as (13) is used to update the state covariance estimation.

In plain language, the problem of the conventional framework originates from the assumption that the selected Kalman gain is optimal. However, the Kalman gain, which was optimized based on the approximated measurement function near the predicted states, generally will not minimize the trace of the actual covariance. The reason is that the actual states can be far from the predicted states and the approximations made in the "predict" step may be inaccurate. An example of such a problem is shown in Fig. 1, where we use an EKF to estimate a plane's position. In the example, the state is the plane's position along the x-axis, and the measurement function is the altitude of the ground beneath the plane, which is a nonlinear function of the state. Due to the inaccurate approximation of the measurement function around the predicted state (the dashed purple line, "Approx. 1", in Fig. 1), the EKF overestimates the position of the plane, and the absolute value of the state estimation error  $|x_k-\hat{x}_{k|k}|$  becomes higher after the "update" step. Meanwhile, the estimated standard deviation of the state,  $\sigma_{k|k}$ , becomes smaller after the "update" step. Such a contradiction suggests that the effectiveness of the Kalman gain is overestimated. This is visualized by the narrow yellow distribution in the "update" step in Fig. 1, which does not cover the true state.

## 2.3 The proposed new framework for nonlinear Kalman filters

Once we fundamentally understand the problem of the conventional framework, the solution is simple. We can redo the approximation after the update and use the newly approximated measurement function to update

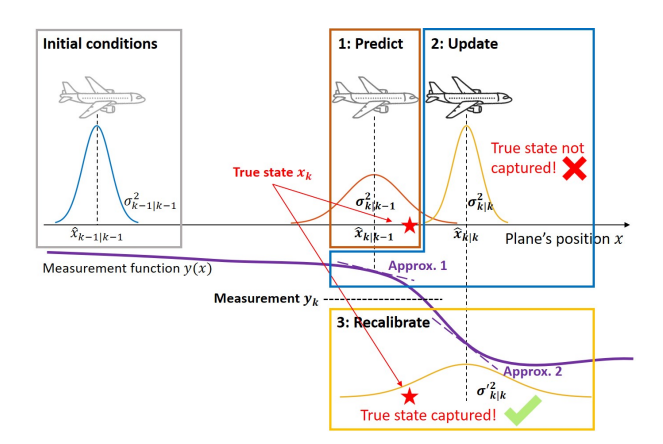


Fig. 1. The basic idea of the new framework for nonlinear KFs. The additional step we propose re-approximates the nonlinear measurement function around the updated states, making the final covariance estimation more accurate.

the covariance estimation. In our new framework, this new step is called "recalibrate". As shown in Fig. 1, with this additional step, the estimated covariance matrix may not have the smallest possible trace after the update; instead, it will honestly reflect the effect of the Kalman gain on the actual state covariance matrix. This is visualized by the wider yellow distribution in the "recalibrate" step, which now covers the true state.

Mathematically, "recalibrate" means to re-approximate the measurement functions around the updated states  $\hat{x}_{k|k}$  and re-estimate the matrices  $P_{z,k}, S_k$  and  $P_{xz}$ . We denote these re-approximated covariance matrices as  $P_{z,k|k}, S_{k|k}$ , and  $P_{xz,k|k}$  since they are all estimated based on the updated states. Similar to (11), these covariance matrices are calculated by

$$\begin{cases}
P_{z,k|k} := \Phi_y(h; \hat{x}_{k|k}, P_{k|k-1, \text{est}}), \\
S_{k|k} := P_{z,k|k} + R_k, \\
P_{xz,k|k} := \Phi_{xy}(h; \hat{x}_{k|k}, P_{k|k-1, \text{est}}).
\end{cases} (24)$$

In the new framework, the state covariance matrix is updated by replacing  $S_k$  with  $S_{k|k}$  and  $P_{xz,k}$  with  $P_{xz,k|k}$  in (14):

$$P_{k|k,\text{est,new}} = P_{k|k-1,\text{est}} + K_{k,\text{est}} S_{k|k} K_{\text{est}}^{T} - P_{xz,k|k} K_{\text{est}}^{T} - K_{k,\text{est}} P_{xz,k|k}^{T}$$

$$= P_{k|k-1,\text{est}} + P_{xz,k|k-1} S_{k|k-1}^{-1} S_{k|k} S_{k|k-1}^{-1} P_{xz,k|k-1}^{T} - P_{xz,k|k} S_{k|k-1}^{-1} P_{xz,k|k}^{T}.$$

$$- P_{xz,k|k} S_{k|k-1}^{-1} P_{xz,k|k-1}^{T} - P_{xz,k|k-1} S_{k|k-1}^{-1} P_{xz,k|k}^{T}.$$

$$(25)$$

In the new framework, the covariance estimation error after the state update can then be calculated as

$$P_{k|k,\text{err,new}} := P_{k|k,\text{ac}} - P_{k|k,\text{est,new}}. \tag{26}$$

The change in the covariance estimation error after the

update is

$$\Delta P_{k|k,\text{err,new}} := P_{k|k,\text{err}} - P_{k|k-1,\text{err,new}} 
= P_{k|k,\text{ac}} - P_{k|k,\text{est,new}}|_{P_{k|k-1,\text{est}} = P_{k|k-1}}.$$
(27)

Note that the proposed new framework selects the same Kalman gain and does the same state update as the conventional one; the only difference is that the state covariance update equation is now a direct approximation of (14), which is the actual state covariance regardless of the selection of the Kalman gain K. Intuitively, this can prevent the KF from overconfidence because the equation no longer relies on the problematic assumption that the Kalman gain is optimal. To explain this advantage more rigorously, we consider the newly approximated covariance matrices  $P_{z,k|k}$ ,  $S_{k|k}$ , and  $P_{xz,k|k}$  produced by a nonlinear KF as (random) estimators of the actual quantities  $P_{z,k}$ ,  $S_k$ , and  $P_{xz,k}$ . Similar to our previous assumptions about  $P_{z,k|k-1}$ ,  $S_{k|k-1}$ , and  $P_{xz,k|k-1}$ , we regard  $P_{xz,k|k}$  as a random matrix,  $P_{z,k|k}$  as a random positive semidefinite matrix, and  $S_{k|k}$  as a random positive semidefinite matrix. tive definite matrix. Additionally, we assume that these approximated covariance matrices are unbiased estimators and satisfy:

$$\begin{cases}
\mathbb{E}[P_{z,k|k}] = P_{z,k} \\
\mathbb{E}[S_{k|k}] = S_k \\
\mathbb{E}[P_{xz,k|k}] = P_{xz,k}
\end{cases}$$
(28)

With these additional definitions and assumptions, we are able to give the following theorem about the advantage of the new framework:

**Theorem 2** Assume that the conditions (18) and (28) hold. Further assume that the random pair  $(P_{xz,k|k-1}, S_{k|k-1})$  is independent of the random pair  $(P_{xz,k|k}, S_{k|k})$ . Then  $\Delta P_{k|k,\text{err,new}}$ , as defined in (27), satisfies

$$\mathbb{E}\left[\Delta P_{k|k,\text{err,new}}\right] = 0. \tag{29}$$

Consequently, if in addition  $\mathbb{E}[P_{k|k-1,est}] = P_{k|k-1}$ , then  $P_{k|k,est,new}$  calculated in (25) is an unbiased estimator of  $P_{k|k,ac}$ . Namely,

$$\mathbb{E}\left[P_{k|k,\text{est,new}} - P_{k|k,\text{ac}}\right] = 0. \tag{30}$$

**PROOF.** With the assumptions made in Theorem 2, we have:

$$\mathbb{E}[\Delta P_{k|k,\text{err,new}}] \\
= \mathbb{E}[P_{xz,k|k-1}S_{k|k-1}^{-1}(S_{k|k} - S_k)S_{k|k-1}^{-1}P_{xz,k|k-1}^{T}] \\
- \mathbb{E}[(P_{xz,k|k} - P_{xz,k})S_{k|k-1}^{-1}P_{xz,k|k-1}^{T}] \\
- \mathbb{E}[P_{xz,k|k-1}S_{k|k-1}^{-1}(P_{xz,k|k} - P_{xz,k})^{T}] \\
= 0.$$
(31)

The last equality holds because the terms in parentheses are zero, due to the unbiasedness (i.e.,  $\mathbb{E}(S_{k|k}) = S_k$  and  $\mathbb{E}(P_{xz,k|k}) = P_{xz,k}$ ) and independence assumptions.

Theorem 2 suggests that the proposed new framework can generally prevent the filter from being overconfident in the "update" step if the approximation errors of the measurement function at the predicted and updated states are independent of each other. Admittedly, this assumption about the independence of the approximation errors is very hard to verify and may not hold in practice. Nonetheless, the theorem does explain why recalibrating the covariance matrices  $P_{z,k}$ ,  $S_k$ , and  $P_{xz,k}$ after the state update is advantageous for accurate state covariance estimation. Specifically, the advantage comes from our replacement of (13) with (25), which highlights the fundamental idea of the new framework. That is, instead of reducing the updated state covariance matrix to the smallest possible value, we re-approximate the system after the state update to estimate the actual effect of the Kalman gain more accurately.

In nonlinear KFs, the update can sometimes make the state estimate less accurate and increase the actual state covariance, as shown in Fig. 1. If this situation were detectable, a natural reaction would be to withdraw the update and use the more accurate predicted state (and the predicted state covariance) as the final output. Unfortunately, such detection is impossible based solely on the estimated state covariance matrix in the conventional KF framework, since  $P_{k|k,\text{est}}$  calculated in (13) is guaranteed to be smaller than or equal to  $P_{k|k-1,\text{est}}$ . In the new framework, however, the additional "recalibrate" step makes such detection possible, which motivates us to introduce a "back out" step. In general, "back out" means to withdraw unhelpful updates and output the state estimate with a lower estimated mean-squared error. Specifically, by the end of the recalibrate step, the filter has two candidate estimates of the current state: the predicted state  $\hat{x}_{k|k-1}$  with covariance  $P_{k|k-1,\text{est}}$ , and the updated state  $\hat{x}_{k|k}$  with covariance  $P_{k|k,\text{est,new}}$ . Since the trace of the covariance matrix equals the expected squared Euclidean error of the corresponding state estimate, we choose as the final output the estimate whose covariance has the smaller trace. If the "back out" step is omitted, the filter may not only produce a suboptimal estimate, but can also become highly unstable:  $P_{k|k,\text{est,new}}$  computed in (25) is no longer guaranteed to remain bounded by  $P_{k|k-1,\text{est}}$ , and can be several orders of magnitude larger than  $P_{k|k-1,\text{est}}$ , which is clearly undesirable.

The pseudo-code of the new framework is shown in Algorithm 1. Note that the new framework degrades to the conventional framework when the "recalibrate" and "back out" steps are replaced with (13). Moreover, when all measurement functions are linear, the approximations of  $P_{z,k}$ ,  $S_k$ , and  $P_{xz,k}$  become identical

before and after the recalibration step. In this case, the proposed framework is exactly equivalent to the conventional framework and preserves its optimality for linear systems.

 ${\bf Algorithm~1} \ {\bf The~proposed~framework~for~nonlinear} \ {\bf Kalman~filters}$ 

Input: Process noise covariance matrix  $Q_k$ , Measurement noise covariance matrix  $R_k$ , state transition function f(x, u), measurement function h(x), system inputs  $u_k$ , measurements  $z_k$ 

#### Initialization:

16: end for

```
1: \hat{\boldsymbol{x}}_{0|0} = \mathbb{E}[\boldsymbol{x}_0]
  2: P_{0|0} = \mathbb{E}[(\hat{x}_{0|0} - x_0)(\hat{x}_{0|0} - x_0)^T]
  3: for every time step k do
                     Predict:
                     Estimate \hat{\boldsymbol{x}}_{k|k-1} and \boldsymbol{P}_{k|k-1}
  4:
                     (based on \hat{\boldsymbol{x}}_{k-1|k-1}, \boldsymbol{P}_{k-1|k-1}, \boldsymbol{f}, \boldsymbol{u}_k, and \boldsymbol{Q}_k)
                     Update:
  5:
                      Estimate \hat{\boldsymbol{z}}_{k|k-1}, \boldsymbol{P}_{xz,k|k-1} and \boldsymbol{P}_{z,k|k-1}
                     \begin{array}{l} \text{(based on } \boldsymbol{\hat{x}}_{k|k-1}, \boldsymbol{P}_{k|k-1}, \text{ and } \boldsymbol{h}) \\ \boldsymbol{S}_{k|k-1} = \boldsymbol{P}_{z,k|k-1} + \boldsymbol{R}_k \end{array}
  6:
                     egin{align*} m{K}_k &= m{P}_{xz,k|k-1} m{S}_{k|k-1}^{-1} \ m{\hat{x}}_{k|k} &= m{\hat{x}}_{k|k-1} + m{K}_k (m{z}_k - m{\hat{z}}_{k|k-1}) \ m{\hat{z}}_{k|k-1} &= m{\hat{z}}_{k|k-1} + m{K}_k (m{z}_k - m{\hat{z}}_{k|k-1}) \end{aligned}
  7:
  8:
                     Recalibrate:
  9:
                      Estimate P_{xz,k|k} and P_{z,k|k}
                     (based on \hat{\boldsymbol{x}}_{k|k}, \boldsymbol{P}_{k|k-1}, and \boldsymbol{h})
                      egin{aligned} S_{k|k} &= P_{z,k|k} + R_k \ P_{k|k} &= P_{k|k-1} + K_k S_{k|k} K_k^T - P_{xz,k|k} K_k^T - K_k P_{xz,k|k}^T \end{aligned}
10:
11:
                     Back out:
                     \begin{array}{l} \textbf{if} \ \operatorname{tr}(\boldsymbol{P}_{k|k}) > \operatorname{tr}(\boldsymbol{P}_{k|k-1}) \ \textbf{then} \\ \hat{\boldsymbol{x}}_{k|k} = \hat{\boldsymbol{x}}_{k|k-1} \\ \boldsymbol{P}_{k|k} = \boldsymbol{P}_{k|k-1} \\ \textbf{end} \ \textbf{if} \end{array}
12:
13:
14:
15:
```

where,  $\hat{x}$  is the estimated states, P is the states' covariance matrix,  $\hat{z}$  is the estimated measurements,  $P_{xz}$  is the covariance between the states and the measurements,  $P_z$  is the covariance of the estimated measurements, S is the innovation (or residual) covariance,  $K_k$  is the Kalman gain. The subscript k|k-1 represents the estimated value before the state update, and k|k represents the estimated value after the state update.

To provide an intuitive illustration of the roles of the "recalibrate" and "back out" steps, Fig. 2 shows a single update for several nonlinear KFs applied to the scalar measurement model

$$z = h(x) + v$$
,  $h(x) = x^3/3 - x^2/8 - x + 1.5383$ , (32)

with the observed measurement  $z_1 = 0$ . The measurement function h(x) is plotted as the thick gray curve. The predicted state is  $x_{1|0} = 0$  with variance 1.5<sup>2</sup>, and the measurement noise standard deviation is  $\sigma_y = 0.01$ . This example is particularly challenging because  $h'(x_{1|0}) < 0$ 

while the true state lies to the left of  $x_{1|0}$ , so a local linearization can easily mislead the filter. The state and covariance estimates produced by different algorithms are shown in separate rows in the figure. Under the conventional framework, all methods substantially underestimate the actual estimation error, as indicated by the overly narrow  $\pm 1\sigma$  intervals that fail to cover the true state. In contrast, within the proposed framework, the covariance estimates are much more consistent with the true error. In this example, the recalibrated variance correctly indicates that the update is less reliable than the prediction, so the "back out" step is triggered and the filter discards the misleading update, outputting the predicted state and its variance as the final estimate. If the "back out" step is removed from the framework, the estimated state becomes less accurate for all filters. Moreover, in this example, the CKF's estimated variance after the recalibration is approximately 144<sup>2</sup>, which is almost 10,000 times larger than the variance of the predicted state. Such a "covariance explosion" further underscores the necessity of the "back out" step.

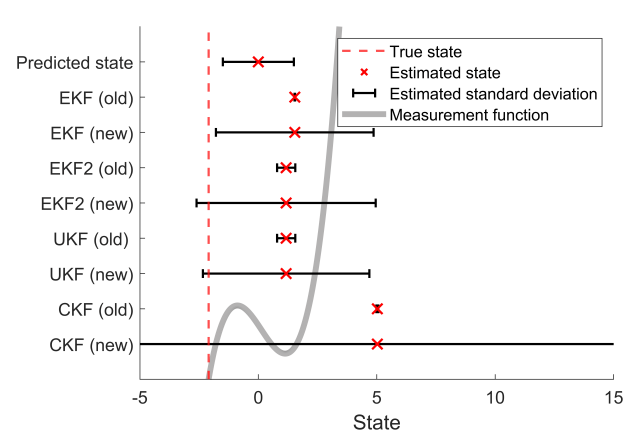


Fig. 2. The comparison of the variance estimation after the state update and recalibration using different frameworks and different types of nonlinear Kalman filters. The recalibrated variance of CKF (new) is approximately  $144^2$ , almost 10,000 times larger than the predicted variance, which underscores the importance of the "back out" step.

Finally, it is insightful to interpret the proposed framework through a machine learning perspective. In the conventional nonlinear KF framework, the Kalman gain is chosen based on approximations constructed around the predicted state. These local approximations can be viewed as an analogue of a "training set": they are reasonably representative of the underlying nonlinear system but do not capture its full complexity. Computing the covariance using the same approximations is then analogous to evaluating an in-sample (training) loss, which tends to be systematically smaller than the true out-of-sample (testing) loss. This offers an intuitive explanation for why the conventional nonlinear KF framework often yields overconfident covariance estimates. In contrast, our new framework computes the covariance based on approximations constructed around the up-

dated state, which can be viewed as an analogue of a "validation set." In this interpretation, Theorem 2 states that, when the information used to design the gain and the information used to assess the covariance are independent, the resulting covariance (or loss) estimate is unbiased. Even though exact independence may not hold in practice, the machine learning literature provides strong empirical evidence that incorporating a validation-like mechanism is effective in mitigating overconfidence (overfitting) and improving estimation accuracy, which is precisely the role played by the "recalibrate" step introduced in this paper. As for the "back out" step, it can be interpreted as reverting to the previous checkpoint when the validation error increases during training, which is also necessary and important for finding the best estimates.

## 2.4 Relationship to Iterated Kalman Filter

The new framework described above may remind the readers of the iterated Kalman filter (IKF), which also re-approximates the measurement function after calculating the Kalman gain [29–31]. However, IKF is fundamentally different from the new framework in three ways. Firstly, IKF redoes the approximation and recalculates the Kalman gain iteratively until convergence. However, such a convergence is not guaranteed, so the algorithm is less robust and often requires finetuning the step size of each iteration [32]. Even if the iteration converges, the convergence may take a very long time. By contrast, the new framework requires no iteration, and the re-approximation is only done once. Secondly, IKF was initially only used on EKF, and the deduction of iterated EKF (IEKF) requires an explicit approximation of the measurement functions (rows 9 and 10 in Algorithm 3 in Appendix C), which is only possible for EKF and EKF2. Although a few attempts have been made to extend IKF to UKF and CKF [30, 31, 33, 34], a consensus on how to do this robustly has not been reached. Therefore, it is not easy to implement IKF on all types of nonlinear KFs while guaranteeing that the estimator can converge in most cases. Our framework, on the other hand, does not have this problem since there is no convergence issue. Thirdly, and most importantly, the basic idea behind IKF is still to find the optimal Kalman gain and not to estimate the covariance matrix accurately. Namely, IKF always updates the states and covariance matrix simultaneously using (13), resulting in overconfident state estimations. When the algorithm cannot converge properly, the estimation can be even worse because the estimated  $P_{z,k}$ ,  $S_k$ , and  $P_{xz,k}$  can be less accurate, which can lead to a higher degree of overconfidence. In general, in terms of making a more accurate estimation, finding the optimal Kalman gain is not as important as making the covariance estimation accurate, as we will show later in the simulation results.

Since IKF also uses (13) to update the state covariance

matrix, it can also be considered as another framework for nonlinear KFs that is similar to the conventional framework. A natural question is: can we combine the new framework with the IKF to get a higher estimation accuracy? Unfortunately, the answer is no because a prerequisite for the new framework to give accurate covariance estimation is that the approximations made at the predicted states  $(P_{z,k|k-1}, S_{k|k-1}, \text{ and } P_{xz,k|k-1})$ are independent of the approximations made at the updated states  $(P_{z,k|k}, S_{k|k}, \text{ and } P_{xz,k|k})$ . However, after IKF converges, these two sets of approximations become the same, which violates this prerequisite in Theorem 2. For example, the IEKF algorithm shown in Algorithm 3 approximates the measurement function iteratively at  $x_{i-1}$  (rows 9-13). When the algorithm converges, in the final iteration, we have  $x_{i-1} \approx x_i = \hat{x}_{k|k}$ , meaning that the approximation of the measurement functions in the final iteration will stay the same after the state update. In fact, to the best of our knowledge, IKF-related algorithms are the only existing types of nonlinear KFs that can not get large benefits from the proposed framework. Nevertheless, for any type of nonlinear KF that can be combined with IKF, its accuracy can be greatly improved when it is combined with our new framework instead. In this sense, we can still say that all existing types of nonlinear KFs can benefit from the proposed framework.

#### 3 Results

To demonstrate the effectiveness of the proposed framework, we validate it in five different applications suitable for nonlinear KFs. A brief description of the five applications is presented in Table 1, and a detailed description of the system models and parameter setup can be found in Appendix B. For each scenario, we combine the old and proposed framework with four different types of nonlinear KFs: EKF, EKF2, UKF, and CKF. We also implemente the IEKF for comparison. The detailed EKF, IEKF, EKF2, UKF, and CKF algorithms used in the paper can be found in Algorithms 2–5 in Appendix C. All these nine (4 + 4 + 1) nonlinear KFs are used for state estimation under different measurement noise setups (the covariance of the measurement noises differs in different setups). To ensure a fair comparison and reduce the impact of Monte Carlo randomness, each KF is simulated 10,000 times for each measurement-noise level. All filters share the same realizations of the random initial state errors, process noises, and measurement noises. Concretely, these random sequences are generated from the same random seed so that the  $i^{th}$  simulation of each method (e.g., EKF, UKF, CKF) is driven by identical noise realizations.

## 3.1 State estimation accuracy

The root mean squared error (RMSE) of the state estimations given by different nonlinear KFs are shown

Table 1 A brief description of the five applications of nonlinear Kalman filters investigated in this paper.

Applications	3D target	Terrain-referenced	Synchronous generator	Pendulum state	Battery state
	tracking	navigation	state estimation	estimation	estimation
Number of states	6	2	4	2	3
Linear state transition function?	Yes	Yes	No	No	No
Number of measurements	2	1	1	1	1
Linear measurement functions?	No	No	No	No	No
Number of inputs	3	2	3	1	1
Number of iterations	30	100	100	100	180

in Figs. 3–7. In all figures, different types of nonlinear KFs are represented by different colors and markers, and the old and new frameworks are represented by dotted lines and solid lines, respectively. The x-axis represents the standard deviations of the measurements. The root mean squared error is calculated from the estimation errors in 10,000 simulations. The estimation error is calculated as the difference between the estimated state and the true state at the end of the final iteration of each simulation. Note that we only show the RMSE of two representative states for systems with more than two states. For example, in 3D target tracking, the six states are the object's speed and position along the three axes, and Fig. 3 examines the object's speed and position estimation accuracy along the x-axis. As can be seen from the five figures, the simulation results are very similar to each other. Therefore, we mainly analyze the first application, 3D target tracking, in depth in this section.

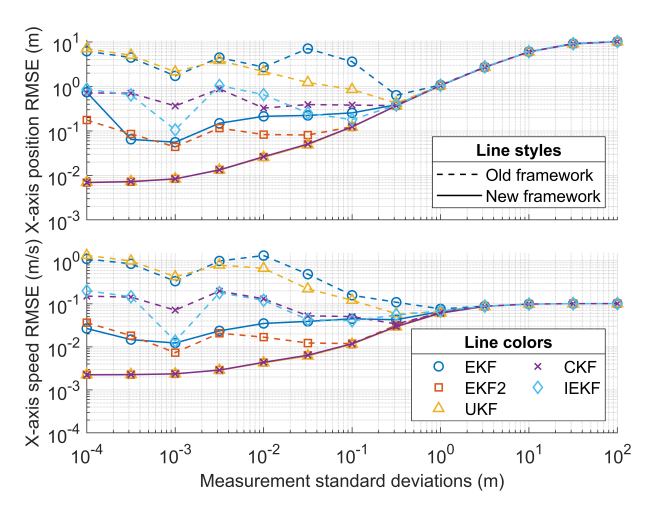


Fig. 3. The root mean squared error of the state estimations under different measurement noise setups (3D target tracking).

As shown in Fig. 3–7, the proposed framework (solid lines) significantly improves the accuracy of all types of nonlinear KFs. The improvement becomes stronger as the measurement noise becomes smaller. This result aligns with our expectations because the proposed framework only changes how the measurements are used

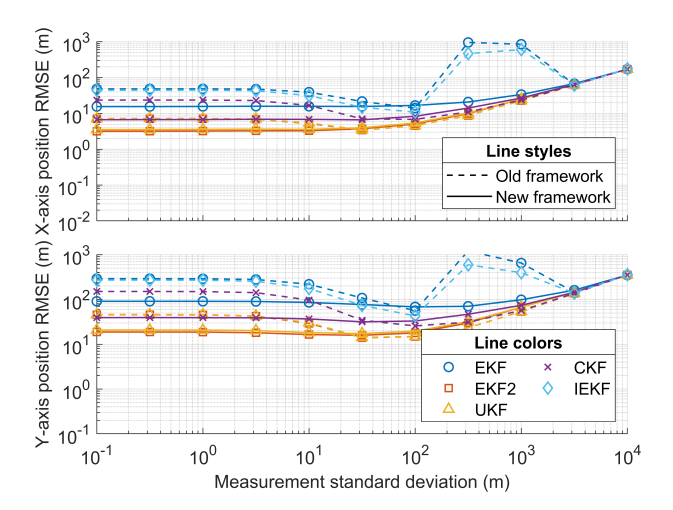


Fig. 4. The root mean squared error of the state estimations under different measurement noise setups (terrain-referenced navigation).

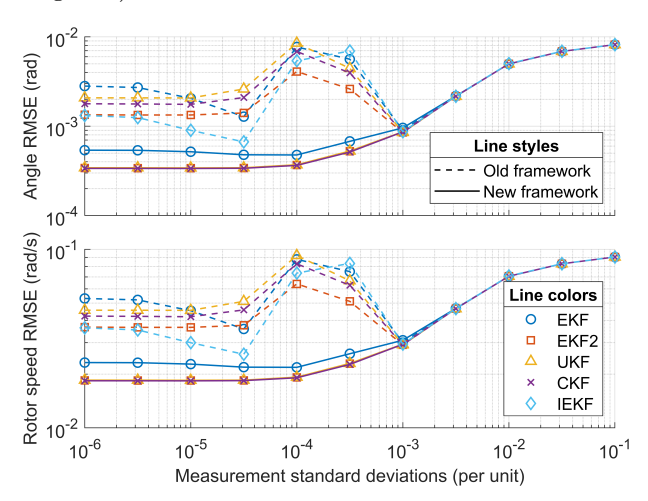


Fig. 5. The root mean squared error of the state estimations under different measurement noise setups (synchronous generator state estimation).

in the nonlinear KF, and the estimations will rely more on the measurements instead of system knowledge as the measurement noise decreases. For all these applications, when the standard deviations of the measurements are small, the RMSE of all four types of nonlinear KFs can

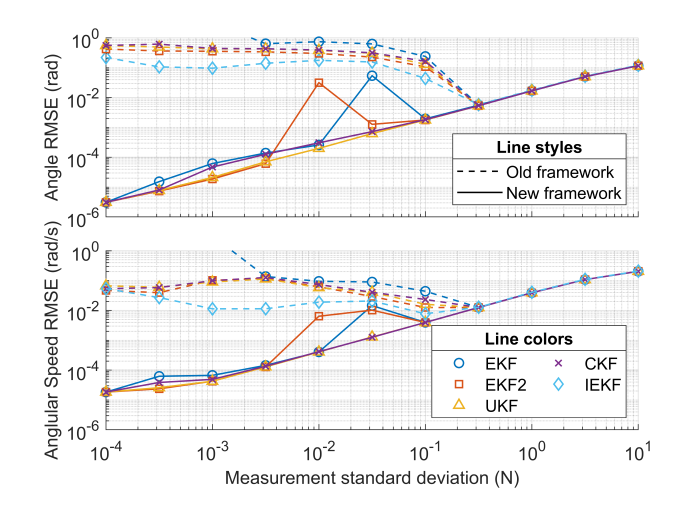


Fig. 6. The root mean squared error of the state estimations under different measurement noise setups (pendulum state estimation).

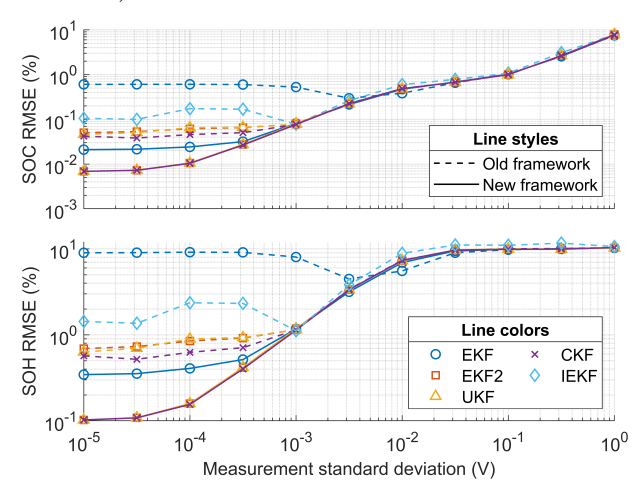


Fig. 7. The root mean squared error of the state estimations under different measurement noise setups (battery state estimation).

usually be reduced by more than an order of magnitude, which is a significant improvement.

Another interesting observation of Figs. 3–7 is that the RMSE of EKF2, UKF, and CKF becomes quite similar after the new framework is used. This phenomenon can be explained by the fact that all three methods consider the first and second-order terms in the Taylor expansion of the nonlinear state transition and measurement functions in certain ways [9]. On the other hand, EKF is generally slightly worse than the other three types of nonlinear KFs because it only considers the first-order terms in the Taylor expansion.

By comparing the performance of IEKF and EKF (with and without the proposed framework) in Figs. 3–7, we observe that although the IEKF outperforms the EKF under the conventional framework, it is consistently inferior to the EKF implemented with the new framework,

while also incurring higher computational cost. As discussed in the Introduction, this discrepancy arises because the IEKF continues to produce overconfident covariance estimates, particularly in cases where the iteration fails to converge — a situation that occurs frequently in practice.

The necessity of the "back out" step is illustrated in Fig. 8, which compares the RMSEs of pendulum state estimation (Application 3) with and without this step. The results show that, without the "back out" step, all four nonlinear KF variants become significantly less accurate when the measurement noise is low. This degradation can be attributed to the fact that the a posteriori covariance computed in (25) is not guaranteed to be bounded. As illustrated previously in Fig. 2, without the "back out" step, the covariance may grow explosively, leading to severely inaccurate state estimates in subsequent iterations. It should be noted, however, that the impact of the "back out" step is application dependent. For example, as shown in Fig. 9, removing this step in Application 1 noticeably degrades only the EKF performance, while EKF2, UKF, and CKF are almost unaffected. Nevertheless, it is still advisable to retain this step to guard against potential covariance explosion, since it incurs negligible computational overhead in the proposed framework. Appendix D presents the corresponding results for the other applications and reports, for all five applications, the percentage of update steps in which the "back out" mechanism is actually triggered.

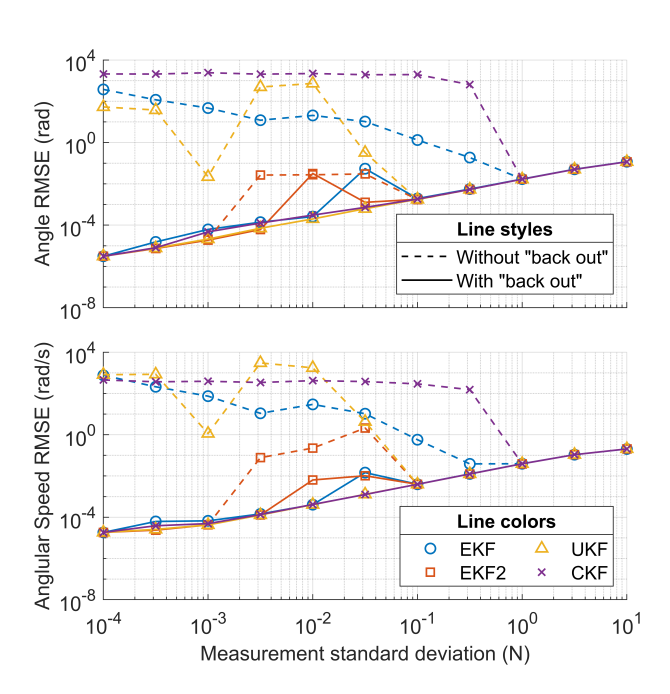


Fig. 8. The root mean squared error of the state estimations with and without the "back out" step under different measurement noise setups (pendulum state estimation).

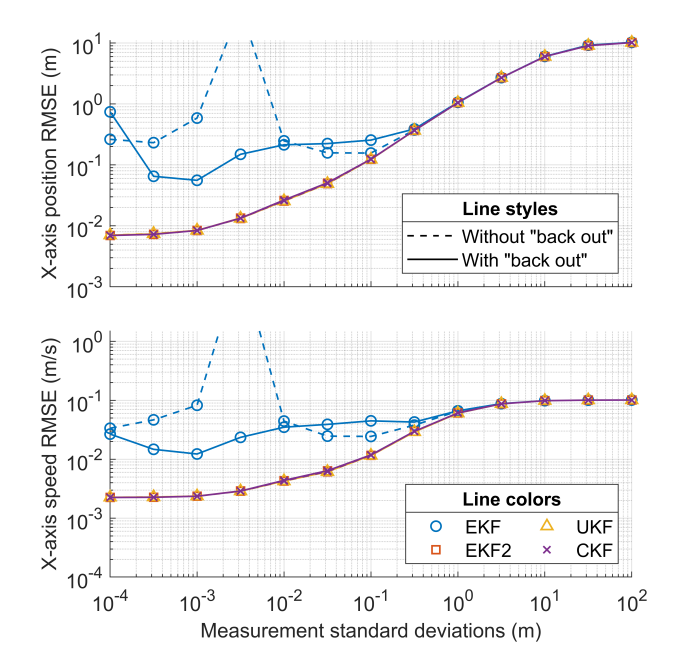


Fig. 9. The root mean squared error of the state estimations with and without the "back out" step under different measurement noise setups (3D target tracking).

## 3.2 Covariance estimation accuracy

As discussed previously, the proposed framework aims to improve covariance estimation by re-approximating the measurement functions after each state update. To evaluate whether the framework actually leads to more accurate covariance estimates, we introduce two metrics for assessing covariance estimation accuracy: the Average Normalized Estimation Error Squared (ANEES) and the Noncredibility Index (NCI). Specifically, the ANEES at time step k is defined as [35]:

$$ANEES_k := \frac{1}{n_x N_{MC}} \sum_{i=1}^{N_{MC}} (x_k^{(i)} - \hat{x}_{k|k}^{(i)})^T (P_{k,est}^{(i)})^{-1} (x_k^{(i)} - \hat{x}_{k|k}^{(i)}),$$
(33)

where  $n_x$  is the state dimension and  $N_{\rm MC}=10{,}000$  is the number of Monte Carlo simulations. The superscript (i) denotes the  $i^{\rm th}$  Monte Carlo simulation. Here,  $x_k^{(i)}$  and  $\hat{x}_{k|k}^{(i)}$  are the true and estimated states at time step k, respectively, and  $P_{k,\rm est}^{(i)}$  is the corresponding state estimation error covariance matrix. Note that  $P_{k,\rm est}^{(i)}=P_{k|k-1,\rm est}^{(i)}$  for the conventional framework, whereas  $P_{k,\rm est}^{(i)}=P_{k|k,\rm est}^{(i)}$  for the proposed frame-

work. When  $P_{k,\text{est}}^{(i)}$  equals the true error covariance and the estimation error is zero-mean Gaussian, we have  $\mathbb{E}[\text{ANEES}_k] = 1$ . Therefore, the deviation of  $\text{ANEES}_k$  from 1 reflects the degree of overconfidence or conservatism in the KF. However, since the estimation error can be biased and non-Gaussian in practice, the value of ANEES alone may not be a sufficiently reliable indicator of overconfidence [35]. Therefore, we also consider the metric NCI, which quantifies the mismatch between the estimated covariance and the empirical covariance

of the estimation error. Specifically, the NCI at time step k is defined as [36]:

$$NCI_{k} := \frac{10}{N_{MC}} \sum_{i=1}^{N_{MC}} \log_{10} \frac{\left(x_{k}^{(i)} - \hat{x}_{k|k}^{(i)}\right)^{T} \left(P_{k, est}^{(i)}\right)^{-1} \left(x_{k}^{(i)} - \hat{x}_{k|k}^{(i)}\right)}{\left(x_{k}^{(i)} - \hat{x}_{k|k}^{(i)}\right)^{T} \left(P_{k}^{*}\right)^{-1} \left(x_{k}^{(i)} - \hat{x}_{k|k}^{(i)}\right)}, \tag{34}$$

where  $P_k^*$  is the sample error covariance at time step k, defined by

$$P_k^* := \frac{1}{N_{\text{MC}}} \sum_{i=1}^{N_{\text{MC}}} \left( x_k^{(i)} - \hat{x}_{k|k}^{(i)} \right) \left( x_k^{(i)} - \hat{x}_{k|k}^{(i)} \right)^T. \tag{35}$$

By construction,  $NCI_k \approx 0$  when  $P_{k,est}^{(i)}$  matches  $P_k^*$ ,  $NCI_k > 0$  indicates overconfidence, and  $NCI_k < 0$  indicates conservatism. Given the definitions of ANEES and NCI for each step k, we define the global ANEES and NCI as the average across all time steps:

$$\begin{cases} \text{ANEES} = \frac{1}{N_{\text{step}}} \sum_{k=1}^{N_{\text{step}}} \text{ANEES}_k, \\ \text{NCI} = \frac{1}{N_{\text{step}}} \sum_{k=1}^{N_{\text{step}}} \text{NCI}_k, \end{cases}$$
(36)

where  $N_{\text{step}}$  is the total number of time steps in the simulation. Given these metrics, Fig. 10 compares the global ANEES and NCI of various KF algorithms using the conventional and proposed frameworks in the target tracking application. Under the conventional framework, when the standard deviations of both measurements are below 0.1 m, all nonlinear KFs substantially underestimate the covariance, regardless of the specific algorithm. In contrast, under the proposed framework, only the EKF remains noticeably overconfident, while the ANEES and NCI of the other nonlinear KFs are very close to one and zero, respectively. This residual gap for the EKF is consistent with its neglect of second- and higher-order terms in the measurement functions; nevertheless, its covariance estimates are still significantly more accurate when combined with the proposed frame-

In Fig. 11, we compare the estimated standard deviation of the first state  $\hat{\sigma}_1$  using different KF variants and frameworks in the target tracking application. Specifically,  $\hat{\sigma}_1$  is defined as the estimated posterior standard deviation of the x-axis position in the final iteration, averaged over all Monte Carlo simulations. Mathematically,

$$\hat{\sigma}_1 := \frac{1}{N_{\text{MC}}} \sum_{i=1}^{N_{\text{MC}}} \sqrt{P_{N_{\text{step}},\text{est}}^{(i)}(1,1)}.$$
 (37)

Interestingly, Fig. 11 suggests that the estimated standard deviation is almost the same for both frameworks,

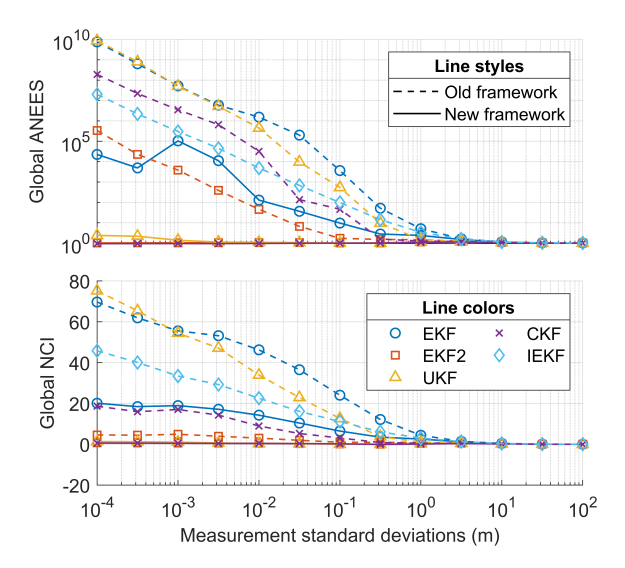


Fig. 10. The global Average Normalized Estimation Error Squared (ANEES) and Noncredibility Index (NCI) of various nonlinear Kalman filters under different measurement noise setups. The new framework significantly mitigates the problem of overconfidence.

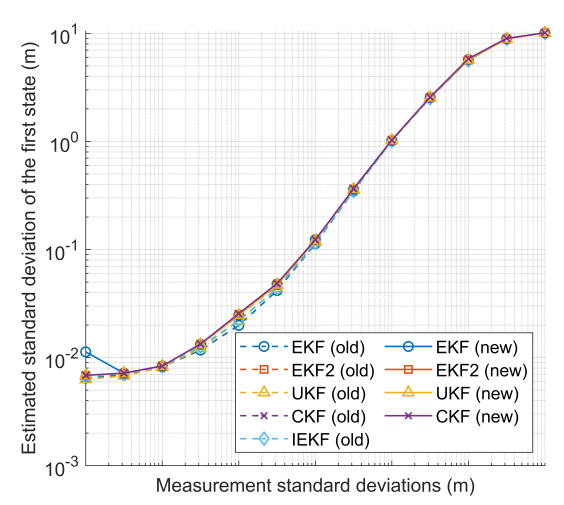


Fig. 11. Estimated standard deviation of the first state for various nonlinear Kalman filters under different measurement noise setups.

regardless of the KF algorithm. These results support the conclusion discussed in Section 2.4: the key to achieving more accurate state estimation is to reduce the gap between the estimated covariance and the actual covariance, rather than merely finding a better Kalman gain that minimizes the estimated covariance.

#### 3.3 Convergence characteristics

Another important metric for evaluating the performance of different filters is the convergence characteristics. We visualize this metric by fixing the standard deviations of the two measurements to 0.01 m and plotted the RMSE of the state estimations after different

numbers of iterations. The results are shown in Fig. 12. From the figure, we can see that all types of nonlinear KFs can converge faster after being combined with the new framework. This result suggests that the proposed framework is very suitable for applications that require high convergence speed.

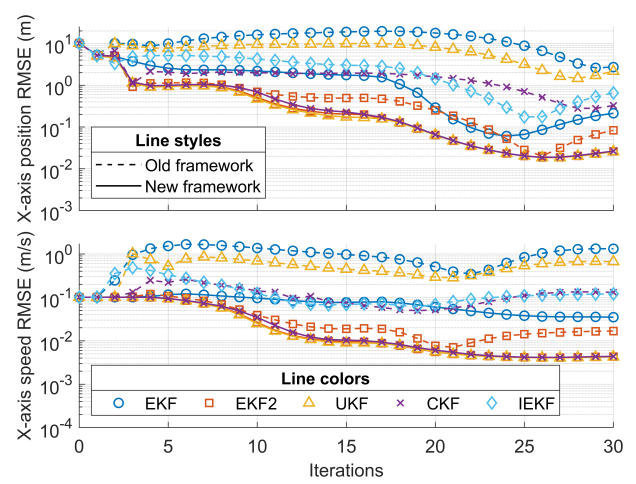


Fig. 12. The root mean squared error of the state estimations after different numbers of iterations.

## 3.4 Computational time

Since the extra steps introduced in the new framework take time, it is also important to compare the computational time of the two frameworks. The results are summarized in Fig. 13. Note that the average runtime shown in the figure is calculated from over 100,000 simulations run on the same computer. Specifically, for each combination of nonlinear KF and framework, we record the method's runtime whenever it was used and calculated the average. After the average runtime is calculated, the value is normalized with respect to the average runtime of the conventional EKF for the same application. In other words, the normalized average runtime of "EKF (old)" always equals one in Fig. 13.

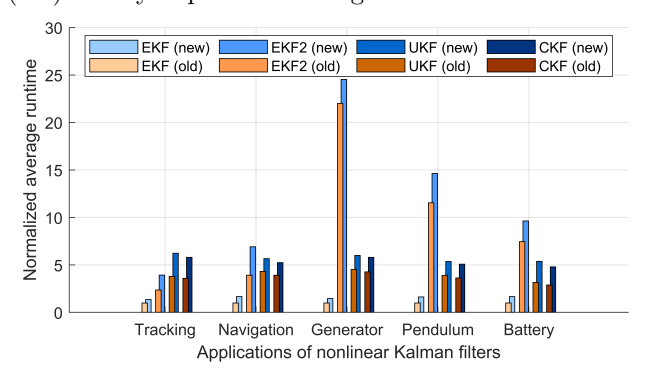


Fig. 13. Comparison of the normalized computational time of different methods and frameworks.

From the result, we can see that the new framework generally increases the computational time by 10–90%,

varying for different nonlinear systems. Namely, when the system has linear state transition functions and nonlinear measurement functions (which is true for the first two applications in the table), the "update" step should be accountable for most of the computational time in the conventional framework and re-approximating the measurement functions can almost double the runtime in the worst case. However, noticing that the new framework can reduce the estimation error by more than an order of magnitude when the measurement noise is small, we can say that the extra computational complexity is generally worth it. Another thing to note is that the combination of EKF and the new framework requires significantly less computational time than the combination of any other nonlinear KFs and the old framework. At the same time, the former's accuracy is generally higher than the latter in the applications we examined in this paper. Therefore, even in situations where the computational time is of major concern, the proposed framework can still be helpful because the new EKF can outperform the old EKF2, UKF, and CKF, in addition to saving a lot of computational time.

#### 4 Conclusion

In this paper, we propose a new framework that can be applied to all types of nonlinear KFs. The new framework re-approximates the measurement functions after the state update, solving the problem of overconfident state covariance estimation, which is an inherent problem in the conventional framework for nonlinear KFs. The new framework was tested in five different applications, reducing the estimation errors by more than an order of magnitude when the measurement noise is low and significantly reducing the convergence time of the algorithm. Considering that all types of sensors will become increasingly more accurate in the future, the proposed framework is expected to bring greater benefits for all kinds of nonlinear KFs over time.

The main limitation of this work is that the proposed framework can only be used in discrete-time nonlinear KFs. For continuous-time nonlinear KFs, the state estimations change continuously over time, so the problem of overconfident covariance estimation does not exist. However, all digital sensors in real life give discrete-time measurements. Even though it is possible to make the signals continuous through interpolation, the continuous-time state estimation problem sometimes includes several partial differential equations, so it is hard and takes a long time to solve [37]. Therefore, most applications of nonlinear KFs in real life use the discrete-time form, and they can all benefit from the new framework proposed in this paper.

#### Acknowledgements

This material is based upon work supported, in part, by the National Science Foundation under Grant No. 1847177.

#### References

- [1] Brian DO Anderson and John B Moore. Optimal filtering. Courier Corporation, 2005.
- [2] Dah-Jing Jwo and Ta-Shun Cho. Critical remarks on the linearised and extended kalman filters with geodetic navigation examples. *Measurement*, 43(9):1077–1089, 2010.
- [3] Thao Tran Phuong, Kiyoshi Ohishi, Chowarit Mitsantisuk, Yuki Yokokura, Kouhei Ohnishi, Roberto Oboe, and Asif Sabanovic. Disturbance observer and kalman filter based motion control realization. *IEEJ Journal of Industry Applications*, 7(1):1–14, 2018.
- [4] Emery N Brown and Christopher H Schmid. [9] application of the kalman filter to computational problems in statistics. In Methods in enzymology, volume 240, pages 171–181. Elsevier, 1994
- [5] Michael Roth, Gustaf Hendeby, Carsten Fritsche, and Fredrik Gustafsson. The ensemble kalman filter: a signal processing perspective. EURASIP Journal on Advances in Signal Processing, 2017:1–16, 2017.
- [6] Kumar Pakki Bharani Chandra and Da-Wei Gu. Nonlinear Filtering: Methods and Applications. Springer, 2019.
- [7] A Gelb. Applied Optimal Estimation. MIT Press, 1974.
- [8] Brendan M Quine. A derivative-free implementation of the extended kalman filter. Automatica, 42(11):1927–1934, 2006.
- [9] Fredrik Gustafsson and Gustaf Hendeby. Some relations between extended and unscented kalman filters. IEEE Transactions on Signal Processing, 60(2):545–555, 2011.
- [10] Simon J Julier and Jeffrey K Uhlmann. New extension of the kalman filter to nonlinear systems. In Signal processing, sensor fusion, and target recognition VI, volume 3068, pages 182–193. Spie, 1997.
- [11] Eric A Wan and Rudolph Van Der Merwe. The unscented kalman filter for nonlinear estimation. In Proceedings of the IEEE 2000 adaptive systems for signal processing, communications, and control symposium (Cat. No. 00EX373), pages 153–158. Ieee, 2000.
- [12] Ienkaran Arasaratnam and Simon Haykin. Cubature kalman filters. *IEEE Transactions on automatic control*, 54(6):1254– 1269, 2009.
- [13] Ienkaran Arasaratnam, Simon Haykin, and Robert J Elliott. Discrete-time nonlinear filtering algorithms using gauss– hermite quadrature. Proceedings of the IEEE, 95(5):953–977, 2007.
- [14] Ienkaran Arasaratnam and Simon Haykin. Square-root quadrature kalman filtering. *IEEE Transactions on Signal Processing*, 56(6):2589–2593, 2008.
- [15] Sebastian Thrun. Probabilistic robotics. Communications of the ACM, 45(3):52–57, 2002.
- [16] Shoudong Huang and Gamini Dissanayake. Convergence and consistency analysis for extended kalman filter based slam. *IEEE Transactions on robotics*, 23(5):1036–1049, 2007.

- [17] Simon J Julier and Jeffrey K Uhlmann. A counter example to the theory of simultaneous localization and map building. In Proceedings 2001 ICRA. IEEE International Conference on Robotics and Automation (Cat. No. 01CH37164), volume 4, pages 4238–4243. IEEE, 2001.
- [18] R Havangi. Robust slam: Slam base on h-infinity square root unscented kalman filter. *Nonlinear Dynamics*, 83(1):767–779, 2016
- [19] Mark R Morelande and Angel F Garcia-Fernandez. Analysis of kalman filter approximations for nonlinear measurements. *IEEE Transactions on Signal Processing*, 61(22):5477–5484, 2013.
- [20] Li Hui-Ping, Xu De-Min, YAO Yao, et al. Consistency analysis of ekf-based slam by measurement noise and observation times. Acta Automatica Sinica, 35(9):1177–1184, 2009
- [21] Shiyuan Wang, Wanli Wang, Badong Chen, and K Tse Chi. Convergence analysis of nonlinear kalman filters with novel innovation-based method. *Neurocomputing*, 289:188– 194, 2018.
- [22] Neil Chada and Xin Tong. Convergence acceleration of ensemble kalman inversion in nonlinear settings. *Mathematics of Computation*, 91(335):1247–1280, 2022.
- [23] Altuğ Aksoy, Fuqing Zhang, and John W Nielsen-Gammon. Ensemble-based simultaneous state and parameter estimation in a two-dimensional sea-breeze model. *Monthly weather review*, 134(10):2951–2970, 2006.
- [24] Jeffrey L Anderson. An adaptive covariance inflation error correction algorithm for ensemble filters. Tellus A: Dynamic meteorology and oceanography, 59(2):210–224, 2007.
- [25] Patrick N Raanes, Marc Bocquet, and Alberto Carrassi. Adaptive covariance inflation in the ensemble kalman filter by gaussian scale mixtures. Quarterly Journal of the Royal Meteorological Society, 145(718):53–75, 2019.
- [26] Kumar Pakki Bharani Chandra and Da-Wei Gu. Nonlinear filtering. Cham, Switzerland: Springer, 2019.
- [27] Daisuke Hotta and Yoichiro Ota. Why does enkf suffer from analysis overconfidence? an insight into exploiting the everincreasing volume of observations. *Quarterly Journal of the Royal Meteorological Society*, 147(735):1258–1277, 2021.
- [28] Kai Xiong, HY Zhang, and CW Chan. Performance evaluation of ukf-based nonlinear filtering. Automatica, 42(2):261–270, 2006.
- [29] Bradley M Bell and Frederick W Cathey. The iterated kalman filter update as a gauss-newton method. *IEEE Transactions* on Automatic Control, 38(2):294–297, 1993.
- [30] Ronghui Zhan and Jianwei Wan. Iterated unscented kalman filter for passive target tracking. IEEE Transactions on Aerospace and Electronic Systems, 43(3):1155–1163, 2007.
- [31] Jing Mu and Yuan-li Cai. Iterated cubature kalman filter and its application. In 2011 IEEE International Conference on Cyber Technology in Automation, Control, and Intelligent Systems, pages 33–37. IEEE, 2011.
- [32] Jindřich Havlík and Ondřej Straka. Performance evaluation of iterated extended kalman filter with variable step-length. In *Journal of Physics: Conference Series*, volume 659, page 012022. IOP Publishing, 2015.
- [33] Lubin Chang, Baiqing Hu, Guobin Chang, and An Li. Marginalised iterated unscented kalman filter. IET Control Theory & Applications, 6(6):847–854, 2012.
- [34] Guobin Chang, Tianhe Xu, and Qianxin Wang. Alternative framework for the iterated unscented kalman filter. IET Signal Processing, 11(3):258–264, 2017.

- [35] Markus Walker, Marcel Reith-Braun, and Uwe D Hanebeck. Weaknesses of the anees and new calibration measures for multivariate predictions. *International Conference on Multisensor Fusion and Integration for Intelligent Systems*, 2025.
- [36] X Rong Li and Zhanlue Zhao. Measuring estimator's credibility: Noncredibility index. In 2006 9th International Conference on Information Fusion, pages 1–8. IEEE, 2006.
- [37] Simo Sarkka. On unscented kalman filtering for state estimation of continuous-time nonlinear systems. *IEEE Transactions on automatic control*, 52(9):1631–1641, 2007.
- [38] Youngjoo Kim, Hyochoong Bang, et al. Introduction to kalman filter and its applications. *Introduction and Implementations of the Kalman Filter*, 1:1–16, 2018.
- [39] Esmaeil Ghahremani and Innocent Kamwa. Online state estimation of a synchronous generator using unscented kalman filter from phasor measurements units. *IEEE Transactions on Energy Conversion*, 26(4):1099–1108, 2011.
- [40] Shida Jiang, Junzhe Shi, Manashita Borah, and Scott Moura. Weaknesses and improvements of the extended kalman filter for battery state-of-charge and state-of-health estimation. In 2024 American Control Conference (ACC), pages 1441–1448. IEEE, 2024.

## A Supplementary proof for Theorem 1

**Lemma 3** Let  $(\Omega, \mathcal{F}, \mathbb{P})$  be an underlying probability space. Assume the random column vectors

$$x: \Omega \to \mathbb{R}^n, \ y: \Omega \to \mathbb{R}^n$$

satisfy  $\mathbb{E}[||x||^2] < \infty$  and  $\mathbb{E}[||y||^2] < \infty$  (i.e.,  $x, y \in L^2(\Omega; \mathbb{R}^n)$ ). Then, the operation on  $L^2(\Omega; \mathbb{R}^n)$  by

$$f(u, v) = \mathbb{E}[u^T v]$$

is an inner product on  $L^2(\Omega; \mathbb{R}^n)$ .

**PROOF.** We start by proving that f is well-defined on  $L^2$ . For any  $u, v \in L^2$ , both  $\mathbb{E}[u^T u]$  and  $\mathbb{E}[v^T v]$  are finite. Therefore,  $\mathbb{E}[(u+v)^T(u+v)]$  should also be finite. Notice that

$$\mathbb{E}[(u+v)^T(u+v)] = \mathbb{E}[u^Tu] + \mathbb{E}[v^Tv] + 2\mathbb{E}[u^Tv],$$

we can conclude that  $\mathbb{E}[u^Tv]$  should also be finite. Therefore, f is well-defined on  $L^2$ . Next, to prove that f is an inner product, we need to show that it satisfies symmetry, linearity in the first argument, and positive-definiteness. Symmetry is satisfied because  $\mathbb{E}[u^Tv] = \mathbb{E}[v^Tu]$ . Linearity is satisfied because for any scalars a, b and  $x, y, z \in L^2$ ,

$$\mathbb{E}[(ax + by)^T z] = a\mathbb{E}[x^T z] + b\mathbb{E}[y^T z].$$

Positive-definiteness is satisfied because for any  $x \in L^2$ ,  $\mathbb{E}[x^T x] \geq 0$ , and the equality sign only holds when x = 0 almost surely.

**Lemma 4** Let S be a random symmetric and positive definite matrix whose mean is the identity matrix I. Let v be a random vector whose mean is  $v_0$ . The following inequality holds:

$$\mathbb{E}(\boldsymbol{v}^T \boldsymbol{S}^{-1} \boldsymbol{v}) \ge \boldsymbol{v}_0^T \boldsymbol{v}_0. \tag{A.1}$$

Note that the equality sign only holds when  $S^{-1}v$  is constant almost surely.

**PROOF.** Let  $x := S^{-\frac{1}{2}}v$ ,  $y := S^{\frac{1}{2}}v_0$ . Since v is a random vector with a mean of  $v_0$ , and S is a random symmetric matrix with a mean of the identity matrix,

$$\begin{cases}
\mathbb{E}[\boldsymbol{x}^T \boldsymbol{x}] = \mathbb{E}[\boldsymbol{v}^T \boldsymbol{S}^{-1} \boldsymbol{v}] \\
\mathbb{E}[\boldsymbol{y}^T \boldsymbol{y}] = \mathbb{E}[\boldsymbol{v}_0^T \boldsymbol{S} \boldsymbol{v}_0] = \boldsymbol{v}_0^T \mathbb{E}[\boldsymbol{S}] \boldsymbol{v}_0 = \boldsymbol{v}_0^T \boldsymbol{v}_0 \\
\mathbb{E}[\boldsymbol{x}^T \boldsymbol{y}] = \mathbb{E}[\boldsymbol{v}^T \boldsymbol{v}_0] = \mathbb{E}[\boldsymbol{v}]^T \boldsymbol{v}_0 = \boldsymbol{v}_0^T \boldsymbol{v}_0
\end{cases} (A.2)$$

According to Lemma 3,  $\mathbb{E}[\boldsymbol{x}^T\boldsymbol{y}]$  is an inner product on  $L^2(\Omega;\mathbb{R}^n)$ . Applying Cauchy–Schwarz inequality, we have

$$\mathbb{E}[\mathbf{v}^T \mathbf{S}^{-1} \mathbf{v}] \ge \frac{(\mathbf{v}_0^T \mathbf{v}_0)^2}{\mathbf{v}_0^T \mathbf{v}_0},\tag{A.3}$$

which completes the proof. Note that the equality holds only when  $S^{-1}v$  is constant almost surely.

## B The detailed simulation setup

This paper uses five different applications of nonlinear KFs to test the effectiveness of the new framework: 3D target tracking, terrain-referenced navigation, synchronous generator state estimation, pendulum state estimation, and battery state estimation.

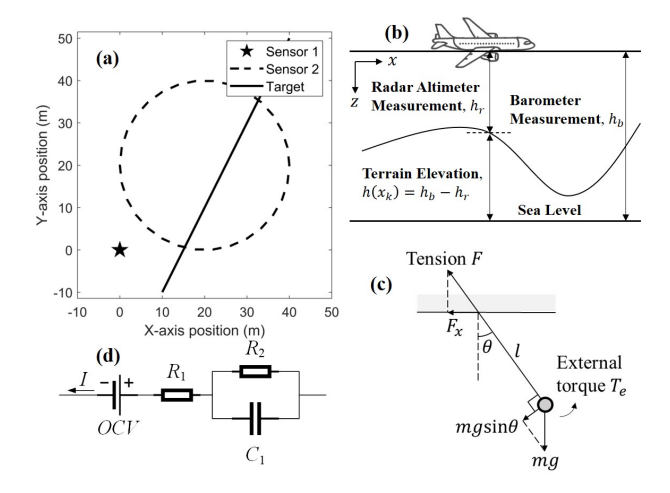


Fig. B.1. Examples of nonlinear systems used in this paper for validation. (a) 3D object tracking. (b) Terrain-referenced navigation. (c) Pendulum state estimation. (d) Battery state estimation.

#### B.1 3D target tracking

This example is adapted from Example 3.3.1 in [38]. As shown in Fig. B.1(a), a target moves in 3D space, and two sensors are used to track its location. The first sensor is at the origin, and the second sensor moves in a circle. The second sensor's location  $(x_{s1}, x_{s2}, x_{s3})$  at step k = 1, 2, ..., 30 is represented by

$$\begin{cases} x_{s1,k} = 20 + 20\cos\left(\frac{(k-1)\pi}{15}\right), \\ x_{s2,k} = 20 + 20\sin\left(\frac{(k-1)\pi}{15}\right), \\ x_{s3,k} = 0. \end{cases}$$
(B.1)

The states are the target's positions  $(x_1, x_2, x_3)$  and speeds  $(v_1, v_2, v_3)$  along the three axes. The measurements  $z_1, z_2$  are the distances between the target and the two sensors. The inputs are the target's accelerations along the three axes, which are assumed to be zero in this example. When the time interval is set to  $\Delta t = 1$ s, the system's state transition and measurement functions can be written as (B.2) and (B.3). Note that the noises are omitted in the equations.

$$\begin{bmatrix} x_{1,k} \\ x_{2,k} \\ x_{3,k} \\ v_{1,k} \\ v_{2,k} \\ v_{3,k} \end{bmatrix} = \begin{bmatrix} x_{1,k-1} + v_{1,k-1} \\ x_{2,k-1} + v_{2,k-1} \\ x_{3,k-1} + v_{3,k-1} \\ v_{1,k-1} \\ v_{2,k-1} \\ v_{3,k-1} \end{bmatrix},$$
(B.2)

$$\begin{bmatrix} z_{1,k} \\ z_{2,k} \end{bmatrix} = \begin{bmatrix} \sqrt{\sum_{i=1}^{3} x_{i,k}^2} \\ \sqrt{\sum_{i=1}^{3} (x_{i,k} - x_{si,k})^2} \end{bmatrix}.$$
 (B.3)

The true initial states of the target are  $x_{1,0} = 10, x_{2,0} = -10, x_{3,0} = 50, v_{1,0} = 1, v_{2,0} = 2, v_{3,0} = 0$ ; the initial state covariance matrix  $P_0$  is diagonal, and its diagonal elements are 100, 100, 100, 0.01, 0.01, and 0.01. The initial state estimations are generated randomly from the multivariate Gaussian distribution with covariance  $P_0$  and mean equal to the true initial states. The process noise covariance matrix is also diagonal, and its diagonal values are 0, 0, 0,  $10^{-6}$ ,  $10^{-6}$ , and  $10^{-6}$ .

## B.2 Terrain-referenced navigation

This example is adapted from Example 3.3.2 in [38]. As shown in Fig. B.1(b), a plane flies above an uneven landscape. The states are the planes' positions along the two axes, denoted as  $x_1$  and  $x_2$ . The measurement  $z_k$  is the terrain's elevation at the plane's present location, which, in practice, is calculated as the difference between the barometer and radar altimeter measurements. The plane knows the contour map in advance, so the terrain's elevation can tell the aircraft its possible locations. However, this task is difficult because all the points on a contour line have the same elevation, and system knowledge must be combined for accurate state estimations. The system inputs are the plane's speeds along the x and y axes, which are 0.5 km/s and 0, respectively. When the time interval is set to  $\Delta t=1$ s, the system's state transition and measurement functions can be written as (B.4) and (B.5). Note that all the units for distance in this example are kilometers, and the noises are omitted in the equations.

$$\begin{bmatrix} x_{1,k} \\ x_{2,k} \end{bmatrix} = \begin{bmatrix} x_{1,k-1} + 0.5 \\ x_{2,k-1} \end{bmatrix},$$
 (B.4)

$$z_k = \sin\sqrt{\left(\frac{x_{1,k}}{40}\right)^2 + \left(\frac{x_{2,k}}{40}\right)^2}.$$
 (B.5)

The true initial states of the target are  $x_{1,0}=10$  km,  $x_{2,0}=10$  km; the initial state covariance matrix  $P_0$  is diagonal, and its diagonal elements are both 1 km². The initial state estimations are generated randomly from the multivariate Gaussian distribution with covariance  $P_0$  and mean equal to the true initial states. The process noise covariance matrix is also diagonal, and its diagonal values are both 0.25 m².

## B.3 Synchronous generator state estimation

This example is adapted from a research paper [39]. The system model is precisely the same as in the paper. The states of the system are the rotor angle  $\delta$ , rotor speed  $\Delta \omega$ , the q-axis component of the voltage  $e'_q$ , and the d-axis component of the voltage  $e'_d$ . For simplicity, these states are denoted as  $x_1$  to  $x_4$ . The measurement  $z_k$  is electrical output power. The system's inputs include the mechanical input torque  $T_m$ , the steady-state internal voltage of the armature  $E_{fd}$ , and the terminal bus voltage  $V_t$ . For simplicity, these inputs are denoted as  $u_1$  to  $u_3$ . The time interval is set to  $\Delta t = 0.1$  ms. The input profiles are the same as in the paper, which are:

$$\begin{cases} u_{1,k} = 0.8, \\ u_{2,k} = 2.11 + 0.0002k, \\ u_{3,k} = 1.002. \end{cases}$$
 (B.6)

All the model parameters are selected to be the same as in [39]. The system's state transition and measurement functions can be written as (B.7) and (B.8). Note that

the noises are omitted from the equations.

$$\begin{bmatrix} x_{1,k} \\ x_{2,k} \\ x_{3,k} \\ x_{4,k} \end{bmatrix} = \begin{bmatrix} x_{1,k-1} \\ x_{2,k-1} \\ x_{3,k-1} \\ x_{4,k-1} \end{bmatrix} + \begin{bmatrix} 377x_{2,k-1}\Delta t \\ \frac{\Delta t}{13} \left[ u_{1,k-1} - \frac{u_{3,k-1}x_{3,k-1}\sin x_{1,k-1}}{0.375} \right] \\ \frac{\Delta t}{0.131} \left[ u_{2,k-1} - x_{3,k-1} \right] \\ -\frac{x_{4,k-1}\Delta t}{0.0131} \end{bmatrix} + \begin{bmatrix} 0 \\ \frac{\Delta t}{13} \left[ 0.9215u_{3,k-1}^2 \sin(2x_{1,k-1}) - 0.05x_{2,k-1} \right] \\ -\frac{4.4933\Delta t}{0.131} \left( x_{3,k-1} - u_{3,k-1}\cos x_{1,k-1} \right) \\ \frac{0.6911u_{3,k-1}\sin x_{1,k-1}\Delta t}{0.0131} \end{bmatrix},$$

$$z_k = \frac{u_{3,k-1}x_{3,k}\sin x_{1,k}}{0.375} + 0.9215u_{3,k-1}^2 \sin(2x_{1,k}).$$
(B.7)

The true initial states of the system are  $x_{1,0}=0.4, x_{2,0}=x_{3,0}=x_{4,0}=0$ . The initial state covariance matrix  $P_0$  is diagonal, and its diagonal elements are  $10^{-4}, 10^{-10}, 10^{-4}$ , and  $10^{-4}$ . The initial state estimations are generated randomly from the multivariate Gaussian distribution with covariance  $P_0$  and mean equal to the true initial states. The process noise covariance matrix is also diagonal, and its diagonal values are  $10^{-10}, 10^{-16}, 10^{-10},$  and  $10^{-10}$ .

(B.8)

#### B.4 Pendulum state estimation

As shown in Fig. B.1(c), one end of the pendulum is fixed to the ceiling with a thin rope. The system's states are the pendulum's angular position  $\theta$  and angular speed  $\omega$ . The measurement  $z_k$  is the horizontal component of tension in the rope. The system input is the external torque exerted on the pendulum, which is zero in this example. The mass of the ball is m=1 kg, the length of the rope is l=1 m, and the gravity acceleration is  $g=9.8\text{m/s}^2$ . The time interval is set to  $\Delta t=0.01\text{s}$ . According to Newton's law, when the time interval is small, the system's state transition and measurement functions can be written as (B.9) and (B.10). Note that the noises are omitted in the equations.

$$\begin{bmatrix} \omega_k \\ \theta_k \end{bmatrix} = \begin{bmatrix} \omega_{k-1} - \frac{g}{l}\sin(\theta_{k-1})\Delta t \\ \theta_{k-1} + \omega_{k-1}\Delta t \end{bmatrix}, \quad (B.9)$$

$$z_k = mg\cos\theta_k\sin\theta_k + ml\omega_k^2\sin\theta_k.$$
 (B.10)

The true initial states of the system are  $\omega_0 = 0$ ,  $\theta_0 = \pi/4$ . The initial state covariance matrix  $P_0$  is diagonal, and its diagonal elements are both  $(\pi/18)^2$ . The initial state estimations are generated randomly from the multivariate Gaussian distribution with covariance  $P_0$  and mean equal to the true initial states. The process noise covariance matrix is also diagonal; its diagonal values are  $10^{-10}$  and 0.

## B.5 Battery state estimation

This example is adapted from a research paper [40]. As shown in Fig. B.1(d), a battery can be modeled as several circuit components, including a voltage source OCV (stands for the cell's open-circuit voltage), an internal resistor  $R_1$ , a transfer resistor  $R_2$ , and a capacitor  $C_1$ . A battery's two most important states are its state of charge (SOC) and state of health (SOH). The SOC is the ratio of the battery's remaining capacity to its present maximum capacity, and the SOH is the ratio of the battery's present maximum capacity to its initial maximum capacity. In general, SOC describes the battery's energy level, while SOH describes the battery's aging level. The states of this system are the SOC, SOH, and capacitor voltage  $U_c$ . The measurement  $z_k$  is the battery's terminal voltage. The input is the charging current, which, in this example, is a three-level square wave shown below:

$$I_k = \begin{cases} -2, & 15 < k \le 75, \\ 2, & 105 < k \le 165, \\ 0, & \text{else.} \end{cases}$$
 (B.11)

The battery's initial maximum capacity is  $Q_0=1\,\mathrm{Ah}$ . The parameters in the equivalent circuit model are chosen to be  $R_1=0.01\,\Omega$ ,  $R_2=0.05\,\Omega$ ,  $1/(R_2C_1)=0.008\,\mathrm{s}$ . The OCV is a function of SOC and SOH, and it can be written as:

$$OCV = \sum_{i=0}^{9} \left( \frac{SOH - 0.8}{0.2} a_{100,10-i} + \frac{1 - SOH}{0.2} a_{80,10-i} \right) SOC^{i},$$
(B.12)

where  $a_{100} = [1390.38, -6961.31, 14760.31, -17230.92, 12055.71, -5162.75, 1330.60, -196.37, 15.60, 2.96], <math>a_{80} = [813.94, -4229.96, 9345.49, -11415.38, 8396.15, -3801.07, 1043.09, -165.29, 14.28, 2.96]$ . The time interval is set to  $\Delta t = 1$ s, and the total simulation time is 180 seconds. The system's state transition and measurement functions can be written as (B.13,B.14). Note that the noises are omitted in the equations.

$$\begin{bmatrix} SOC_k \\ U_{c,k} \\ SOH_k \end{bmatrix} = \begin{bmatrix} SOC_{k-1} \\ U_{c,k-1} \exp\left(\frac{-\Delta t}{R_2 C_1}\right) \\ SOH_{k-1} \end{bmatrix} + \begin{bmatrix} I_{k-1} \Delta t \\ \left[1 - \exp\left(\frac{-\Delta t}{R_2 C_1}\right)\right] R_2 I_{k-1} \\ 0 \end{bmatrix}$$
(B.13)

$$z_k = OCV(SOC_k, SOH_k) + U_{c,k} + R_1 I_k \qquad (B.14)$$

The true initial states of the system are  $SOC_0 = 60\%$ ,  $U_{c,0} = 0$ ,  $SOH_0 = 90\%$ . The initial state covariance matrix  $P_0$  is diagonal; its diagonal elements are 0.04,  $10^{-10}$ , and 0.01. The initial state estimations are 80%, 0, and 100%, respectively. The input current is noisy, and its standard deviation is 1 mA. This input

noise is the only source of the process noises. Since the input current also appears in the measurement function, the actual measurement noise is the combination of the measurement noise of the voltmeter and the noise caused by the term  $R_1I_k$  in the measurement function.

## C The detailed algorithm of various nonlinear Kalman filters used in the paper

The detailed algorithms of EKF, IEKF, EKF2, UKF, and CKF with the new framework are shown in Algorithms 2–6. Note that all these algorithms degrade to the conventional framework when the "Recalibrate" and "Back out" steps are replaced by (13).

Algorithm 2 The extended Kalman filter with the new framework

Input: Process noise covariance matrix  $Q_k$ , Measurement noise covariance matrix  $R_k$ , state transition function f(x, u), measurement function h(x), system inputs  $u_k$ , measurements  $z_k$ 

```
Initialization:
```

```
1: \hat{x}_{0|0} = \mathbb{E}[x_0]
  2: P_{0|0} = \mathbb{E}[(\hat{x}_{0|0} - x_0)(\hat{x}_{0|0} - x_0)^T]
3: for every time step k do
                  Predict:
                  4:
   5:
   6:
   7:
  8:
  9:
                  oldsymbol{P}_{xz,k|k-1} = oldsymbol{P}_{k|k-1} oldsymbol{H}_{k|k-1}^T
                   P_{z,k|k-1} = H_{k|k-1}P_{k|k-1}H_{k|k-1}^T
10:
                   S_{k|k-1} = P_{z,k|k-1} + R_k
11:
                 egin{aligned} m{K}_k &= m{P}_{xz,k|k-1} m{S}_{k|k-1}^{-1} \ \hat{m{x}}_{k|k} &= \hat{m{x}}_{k|k-1} + m{K}_k (m{z}_k - \hat{m{z}}_{k|k-1}) \ 	ext{Recalibrate:} \end{aligned}
12:
13:
                  egin{aligned} m{H}_{k|k} &= rac{\partial m{h}}{\partial m{x}} | \hat{m{x}}_{k|k} \ m{P}_{xz,k|k} &= m{P}_{k|k-1} m{H}_{k|k}^T \end{aligned}
14:
15:
                   P_{z,k|k} = H_{k|k} P_{k|k-1} H_{k|k}^T
16:
                   egin{aligned} oldsymbol{S}_{k|k} &= oldsymbol{P}_{z,k|k} + oldsymbol{R}_k \ oldsymbol{P}_{k|k} &= oldsymbol{P}_{k|k-1} + oldsymbol{K}_k oldsymbol{S}_{k|k} oldsymbol{K}_k^T - oldsymbol{P}_{xz,k|k} oldsymbol{K}_k^T - oldsymbol{K}_k oldsymbol{P}_{xz,k|k}^T \end{aligned}
17:
18:
                   \mathbf{\hat{t}} ftr(P_{k|k}) > \mathrm{tr}(P_{k|k-1}) then \hat{m{x}}_{k|k} = \hat{m{x}}_{k|k-1} P_{k|k} = P_{k|k-1} end if
19:
20:
21:
22:
23: end for
```

# D Supplementary results related to the "back out" step

Fig. 8, 9, D.1–D.3 compare the state estimation accuracy with and without the "back out" step. Additionally, Fig.

Algorithm 3 The iterated extended Kalman filter with the old framework

Input: Process noise covariance matrix  $Q_k$ , Measurement noise covariance matrix  $R_k$ , state transition function f(x, u), measurement function h(x), system inputs  $u_k$ , measurements  $z_k$ 

## Initialization:

```
1: \hat{x}_{0|0} = \mathbb{E}[x_0]
  2: \mathbf{P}_{0|0} = \mathbb{E}[(\hat{x}_{0|0} - x_0)(\hat{x}_{0|0} - x_0)^T]
   3: for every time step k do
                  Predict:
                   egin{aligned} oldsymbol{F}_k &= rac{\partial oldsymbol{f}}{\partial oldsymbol{x}}|\hat{oldsymbol{x}}_{k-1|k-1}, oldsymbol{u}_{k-1}, oldsymbol{u}_{k-1} \ \hat{oldsymbol{x}}_{k|k-1} &= oldsymbol{f}(\hat{oldsymbol{x}}_{k-1|k-1}, oldsymbol{u}_{k-1}) \end{aligned}
  4:
  5:
                   P_{k|k-1} = F_k P_{k-1|k-1} F_k^T + Q_k
  6:
                  Update:
  7:
                   \boldsymbol{x}_0 = \boldsymbol{\hat{x}}_{k|k-1}
                   for i = 1 to 1000 do
  8:
                            \begin{split} & \boldsymbol{H}_{k|k-1} = \frac{\partial \boldsymbol{h}}{\partial \boldsymbol{x}}|_{\boldsymbol{x}_{i-1}} \\ & \hat{\boldsymbol{z}}_{k|k-1} = \boldsymbol{h}(\boldsymbol{x}_{i-1}) + \boldsymbol{H}_{k|k-1}(\boldsymbol{x}_{i-1} - \hat{\boldsymbol{x}}_{k|k-1}) \end{split}
  9:
10:
                            \boldsymbol{P}_{xz,k|k-1} = \boldsymbol{P}_{k|k-1} \boldsymbol{H}_{k|k-1}^T
11:
                            P_{z,k|k-1} = H_{k|k-1}P_{k|k-1}H_{k|k-1}^T
12:
                            \boldsymbol{S}_{k|k-1,i} = \boldsymbol{P}_{z,k|k-1} + \boldsymbol{R}_k
13:
                            K_{k,i} = P_{xz,k|k-1} S_{k|k-1,i}^{-1}
14:
                            egin{aligned} & m{x}_i = \hat{m{x}}_{k|k-1} + m{K}_{k,i} (m{z}_k - \hat{m{z}}_{k|k-1}) \ & 	ext{if } i > 1 	ext{ and } ||m{x}_i - m{x}_{i-1}|| > ||m{x}_{i-1} - m{x}_{i-2}|| 	ext{ then} \end{aligned}
15:
16:
                                    egin{aligned} oldsymbol{S}_{k|k-1,i} &= oldsymbol{S}_{k|k-1,i-1} \ oldsymbol{K}_{k,i} &= oldsymbol{K}_{k,i-1} \end{aligned}
17:
18:
                                    \boldsymbol{x}_i = \boldsymbol{x}_{i-1}
19:
20:
                                    break
21:
                             end if
                            if \max_{j} |1 - x_i(j)/x_{i-1}(j)| < 0.001 then
22:
23:
                            end if
24:
25:
                   end for
26:
                   S_{k|k-1} = S_{k|k-1,i}
                   K_k = K_i
27:
28:
                   \hat{m{x}}_{k|k} = m{x}_i
                   P_{k|k} = P_{k|k-1} - K_k S_{k|k-1} K_k^T
29:
30: end for
```

Note that rows 16–21 are added to prevent the state estimations from diverging. Namely, when the sign of divergence is detected (row 16), the newest updates of the states, Kalman gain, and measurement residual covariance matrix are withdrawn (rows 17–19). If such a withdrawal is not made, we find in the simulation that the estimation accuracy can be much lower. This characteristic also suggests that the algorithm is not very robust and stable.

D.4–D.8 quantify how often the proposed "back out" step is activated in practice by reporting the percentage of state updates that trigger this safeguard.

**Algorithm 4** The second-order extended Kalman filter with the new framework

Input: Process noise covariance matrix  $Q_k$ , Measurement noise covariance matrix  $R_k$ , states number  $n_x$ , measurements number  $n_m$ , state transition function f(x, u), measurement function h(x), system inputs  $u_k$ , measurements  $z_k$  Initialization:

```
1: \hat{x}_{0|0} = \mathbb{E}[x_0]
   2: P_{0|0} = \mathbb{E}[(\hat{\boldsymbol{x}}_{0|0} - \boldsymbol{x}_0)(\hat{\boldsymbol{x}}_{0|0} - \boldsymbol{x}_0)^T]
3: for every time step k do
                    Predict:
                     \begin{aligned} & F_k = \frac{\partial f}{\partial x}|_{\hat{x}_{k-1|k-1}, u_{k-1}} \\ & F_{i,k}^* = \left[\frac{\partial^2 f_i}{\partial x_m \partial x_n}|_{\hat{x}_{k-1|k-1}, u_{k-1}}\right]_{mn}, i = 1, \dots, n_x \\ & \hat{x}_{k|k-1} = f(\hat{x}_{k-1|k-1}, u_{k-1}) + \frac{1}{2} \left[ \operatorname{tr}(F_{i,k}^* P_{k-1|k-1}) \right]_i \end{aligned}
   4:
   5:
   6:
                      P_{k|k-1} = F_k P_{k-1|k-1} F_k^T
   7:
                         +\frac{1}{2}\left[\operatorname{tr}(F_{i,k}^*P_{k-1|k-1}F_{i,k}^*P_{k-1|k-1})\right]_{ii}+Q_k
                      oldsymbol{H}_{k|k-1} = rac{\partial oldsymbol{h}}{\partial oldsymbol{x}}|_{\hat{oldsymbol{x}}_{k|k-1}}
   8:
                      \boldsymbol{H}_{i,k|k-1}^* = \left[\frac{\partial^2 h_i}{\partial x_m \partial x_n}|_{\hat{\boldsymbol{x}}_{k|k-1}}\right]_{mn}, i = 1, \dots, n_m
   9:
                      \hat{\boldsymbol{z}}_{k|k-1} = \boldsymbol{h}(\hat{\boldsymbol{x}}_{k|k-1}) + \frac{1}{2} \left[ \operatorname{tr}(\boldsymbol{H}_{i|k|k-1}^* \boldsymbol{P}_{k|k-1}) \right]_i
10:
                      P_{xz,k|k-1} = P_{k|k-1}H_{k|k-1}^T
11:
                      P_{z,k|k-1} = H_{k|k-1}P_{k|k-1}H_{k|k-1}^T
12:
                         + \tfrac{1}{2} \big[ \mathrm{tr}(\boldsymbol{H}_{i,k|k-1}^* \boldsymbol{P}_{k|k-1} \boldsymbol{H}_{j,k|k-1}^* \boldsymbol{P}_{k|k-1}) \big]_{ij}
                      oldsymbol{S}_{k|k-1} = oldsymbol{P}_{z,k|k-1} + oldsymbol{R}_k
13:
                      K_k = P_{xz,k|k-1}S_{k|k-1}^{-1}
14:
                    \hat{m{x}}_{k|k} = \hat{m{x}}_{k|k-1} + m{K}_k(m{z}_k - \hat{m{z}}_{k|k-1})Recalibrate:
15:
                    Recalibration: m{H}_{k|k} = rac{\partial m{h}}{\partial m{x}} |\hat{m{x}}_{k|k} \ m{H}_{i,k|k}^* = \left[ rac{\partial^2 h_i}{\partial x_m \partial x_n} |\hat{m{x}}_{k|k} 
ight]_{mn}, i = 1, \dots, n_m
16:
17:
                      \boldsymbol{P}_{xz,k|k} = \boldsymbol{P}_{k|k-1} \boldsymbol{H}_{k|k}^T
18:
                      oldsymbol{P}_{z,k|k} = oldsymbol{H}_{k|k} oldsymbol{P}_{k|k-1} oldsymbol{H}_{k|k}^T
19:
                           +\frac{1}{2}\left[\operatorname{tr}(\boldsymbol{H}_{i,k|k}^*\boldsymbol{P}_{k|k-1}\boldsymbol{H}_{i,k|k}^*\boldsymbol{P}_{k|k-1})\right]_{i,i}
                      S_{k|k} = P_{z,k|k} + R_k
20:
                      P_{k|k} = P_{k|k-1} + K_k S_{k|k} K_k^T - P_{xz,k|k} K_k^T - K_k P_{xz,k|k}^T
21:
                    Back out:
                      if \operatorname{tr}(\boldsymbol{P}_{k|k}) > \operatorname{tr}(\boldsymbol{P}_{k|k-1}) then
22:
                     \hat{oldsymbol{x}}_{k|k} = \hat{oldsymbol{x}}_{k|k-1} \ oldsymbol{P}_{k|k} = oldsymbol{P}_{k|k-1} \ 	ext{end if}
23:
24:
25:
26: end for
```

# Algorithm 5 The cubature Kalman filter with the new framework

Input: Process noise covariance matrix  $Q_k$ , Measurement noise covariance matrix  $R_k$ , states number  $n_x$ , state transition function f(x, u), measurement function h(x), system inputs  $u_k$ , measurements  $z_k$  Initialization:

```
1: \hat{x}_{0|0} = \mathbb{E}[x_0]
    2: P_{0|0} = \mathbb{E}[(\hat{x}_{0|0} - x_0)(\hat{x}_{0|0} - x_0)^T]
3: for every time step k do
                                Predict:
                                   \boldsymbol{L} = [\boldsymbol{L}_1, \dots, \boldsymbol{L}_{n_x}] = \operatorname{chol}(\boldsymbol{P}_{k-1|k-1}),
    4:
                                 m{L} = [m{L}_1, \dots, m{L}_{n_x}] = \operatorname{chol}(m{F}_{k-1|k-1}), where m{L}m{L}^T = m{P}_{k-1|k-1}

m{\mathcal{X}}_{i,k-1} = \hat{m{x}}_{k-1|k-1} + \sqrt{n_x}m{L}_i, i = 1, \dots, n_x

m{\mathcal{X}}_{i+n_x,k-1} = \hat{m{x}}_{k-1|k-1} - \sqrt{n_x}m{L}_i, i = 1, \dots, n_x

m{\mathcal{X}}_{i,k|k-1}^* = m{f}(m{\mathcal{X}}_{i,k-1}, m{u}_{k-1}), i = 1, \dots, 2n_x
    5:
    6:
    7:
                                 \hat{m{x}}_{k|k-1} = \sum_{i=1}^{2n_x} rac{1}{2n_x} m{\mathcal{X}}_{i,k|k-1}^* \ \hat{m{x}}_{k|k-1} = \sum_{i=1}^{2n_x} rac{1}{2n_x} m{\mathcal{X}}_{i,k|k-1}^* \ m{P}_{k|k-1} = \sum_{i=1}^{2n_x} rac{1}{2n_x} [m{\mathcal{X}}_{i,k|k-1}^* - \hat{m{x}}_{k|k-1}] [m{\mathcal{X}}_{i,k|k-1}^* \ - \hat{m{x}}_{k|k-1}]^T + m{Q}_k
    8:
    9:
                                 Update:
                                   \mathbf{L} = [\mathbf{L}_1, \dots, \mathbf{L}_{n_x}] = \operatorname{chol}(\mathbf{P}_{k|k-1})

\mathbf{X}_{i,k|k-1} = \hat{\mathbf{x}}_{k|k-1} + \sqrt{n_x}\mathbf{L}_i, i = 1, \dots, n_x
10:
11:

\mathcal{X}_{i+n_x,k|k-1}^{i,n_i-1} = \hat{\boldsymbol{x}}_{k|k-1}^{i} + \sqrt{n_x} \boldsymbol{L}_i, i = 1, \dots, n_x \\
\mathcal{Z}_{i,k|k-1} = \hat{\boldsymbol{x}}_{k|k-1}^{i} - \sqrt{n_x} \boldsymbol{L}_i, i = 1, \dots, n_x \\
\mathcal{Z}_{i,k|k-1} = \boldsymbol{h}(\boldsymbol{\mathcal{X}}_{i,k|k-1}), i = 1, \dots, 2n_x

12:
13:
                                egin{align*} oldsymbol{\mathcal{Z}}_{i,k|k-1} &= oldsymbol{h}(oldsymbol{\mathcal{X}}_{i,k|k-1}), i = 1, \dots, 2n_x \ \hat{oldsymbol{z}}_{k|k-1} &= \sum_{i=1}^{2n_x} rac{1}{2n_x} oldsymbol{\mathcal{Z}}_{i,k|k-1} \ P_{xz,k|k-1} &= \sum_{i=1}^{2n_x} rac{1}{2n_x} [oldsymbol{\mathcal{X}}_{i,k|k-1} - \hat{oldsymbol{x}}_{k|k-1}] [oldsymbol{\mathcal{Z}}_{i,k|k-1} \\ &- \hat{oldsymbol{z}}_{k|k-1}]^T \ P_{z,k|k-1} &= \sum_{i=1}^{2n_x} rac{1}{2n_x} [oldsymbol{\mathcal{Z}}_{i,k|k-1} - \hat{oldsymbol{z}}_{k|k-1}] [oldsymbol{\mathcal{Z}}_{i,k|k-1} \\ &- \hat{oldsymbol{z}}_{k|k-1}]^T \ S_{k|k-1} &= P_{z,k|k-1} + R_k \ K_k &= P_{xz,k|k-1} S_{k|k-1}^{-1} \ \hat{oldsymbol{x}}_{k|k-1} + oldsymbol{\mathcal{X}}_{k|k-1} \\ \hat{oldsymbol{x}}_{k|k-1} &= \hat{oldsymbol{x}}_{k|k-1} + oldsymbol{\mathcal{X}}_{k|k-1} \end{aligned}
14:
15:
16:
17:
18:
                                   \hat{m{x}}_{k|k} = \hat{m{x}}_{k|k-1} + m{K}_k(m{z}_k - \hat{m{z}}_{k|k-1})
19:
                                 Recalibrate:
                                   \boldsymbol{\mathcal{X}}_{i,k|k} = \hat{\boldsymbol{x}}_{k|k} + \sqrt{n_x} \boldsymbol{L}_i, i = 1, \dots, n_x
20:
                                  oldsymbol{\mathcal{X}}_{i+n_x,k|k}^{i,n|k} = \hat{oldsymbol{x}}_{k|k} - \sqrt{n_x} oldsymbol{L}_i, i = 1, \dots, n_x
oldsymbol{\mathcal{Z}}_{i,k|k} = oldsymbol{h}(oldsymbol{\mathcal{X}}_{i,k|k}), i = 1, \dots, 2n_x
21:
22:
                                   \hat{oldsymbol{z}}_{k|k} = \sum_{i=1}^{2n_x} rac{1}{2n_x} oldsymbol{\mathcal{Z}}_{i,k|k}
23:
                                  egin{align*} & \mathcal{L}_{i=1}^{i=1} rac{2n_x}{2n_x} rac{1}{1} rac{1}{2n_x} [m{\mathcal{X}}_{i,k|k} - \hat{m{x}}_{k|k}] [m{\mathcal{Z}}_{i,k|k} - \hat{m{z}}_{k|k}]^T \ & m{P}_{z,k|k} = \sum_{i=1}^{2n_x} rac{1}{2n_x} [m{\mathcal{Z}}_{i,k|k} - \hat{m{z}}_{k|k}] [m{\mathcal{Z}}_{i,k|k} - \hat{m{z}}_{k|k}]^T \ & m{S}_{k|k} = m{P}_{z,k|k} + m{R}_k \end{aligned}
24:
25:
26:
                                   P_{k|k} = P_{k|k-1} + K_k S_{k|k} K_k^T - P_{xz,k|k} K_k^T - K_k P_{xz,k|k}^T
27:
                                 Back out:
                                   if \operatorname{tr}(P_{k|k}) > \operatorname{tr}(P_{k|k-1}) then
28:
29:
                                                   \boldsymbol{\hat{x}}_{k|k} = \boldsymbol{\hat{x}}_{k|k-1}
                                                  oldsymbol{P}_{k|k}^{\kappa_{|\kappa}} = oldsymbol{P}_{k|k-1}^{\kappa_{|\kappa|}}
30:
31:
                                   end if
```

32: end for

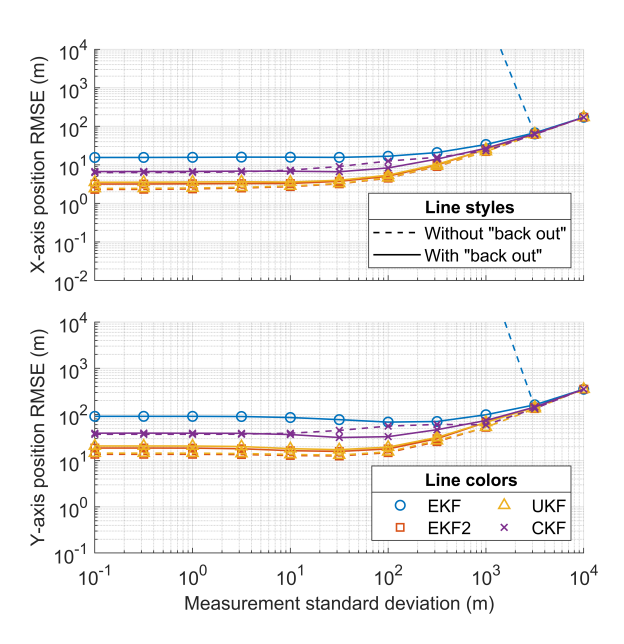


Fig. D.1. The root mean squared error of the state estimations with and without the "back out" step under different measurement noise setups (terrain-referenced navigation).

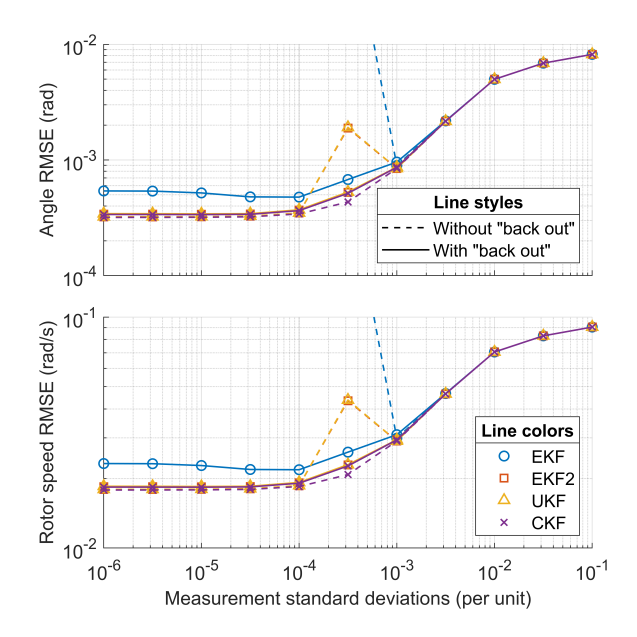


Fig. D.2. The root mean squared error of the state estimations with and without the "back out" step under different measurement noise setups (synchronous generator state estimation).

## Algorithm 6 The unscented Kalman filter with the new framework

Input: Process noise covariance matrix  $Q_k$ , Measurement noise covariance matrix  $R_k$ , states number  $n_x$ , state transition function f(x, u), measurement function h(x), system inputs  $u_k$ , measurements  $z_k$ , hyperparameters  $\alpha = 10^{-3}$ ,  $\beta = 2$ ,  $\kappa = 0$ 

```
Initialization:
```

```
1: \hat{x}_{0|0} = \mathbb{E}[x_0]
  2: \mathbf{P}_{0|0} = \mathbb{E}[(\hat{x}_{0|0} - x_0)(\hat{x}_{0|0} - x_0)^T]
  3: \lambda = \alpha^2 (n_x + \kappa) - n_x
 4: W_i^{(c)} = W_i^{(m)} = 1/(2n_x + 2\lambda), i = 1, \dots, n_x

5: W_0^{(c)} = \lambda/(n_x + \lambda) + 1 - \alpha^2 + \beta

6: W_0^{(m)} = \lambda/(n_x + \lambda)
  7: for every time step k do
                 Predict:
                  L = [L_1, ..., L_{n_x}] = \text{chol}(P_{k-1|k-1}), \text{ where } LL^T = P_{k-1|k-1}
  8:
                  [L_1, ..., L_{n_x}] = i^{th} column of L, i = 1, ..., n_x
  9:
                  \boldsymbol{\mathcal{X}}_{0,k-1} = \boldsymbol{\hat{x}}_{k-1|k-1}
10:
                  \boldsymbol{\mathcal{X}}_{i,k-1} = \hat{\boldsymbol{x}}_{k-1|k-1} + \sqrt{\lambda + n_x} \boldsymbol{L}_i, i = 1, \dots, n_x
11:
                  \boldsymbol{\mathcal{X}}_{i+n_x,k-1} = \hat{\boldsymbol{x}}_{k-1|k-1} - \sqrt{\lambda + n_x} \boldsymbol{L}_i, i = 1,\dots, n_x
12:
                  \mathcal{X}_{i,k|k-1} = f(\mathcal{X}_{i,k-1}, u_{k-1}), i = 0, 1, \dots, 2n_x
13:
                  \hat{\boldsymbol{x}}_{k|k-1} = \sum_{i=0}^{2n_x} W_i^{(m)} \boldsymbol{\mathcal{X}}_{i,k|k-1}
14:
                  m{P}_{k|k-1} = \sum_{i=0}^{2n_x} W_i^{(c)} [m{\mathcal{X}}_{i,k|k-1} - \hat{m{x}}_{k|k-1}] [m{\mathcal{X}}_{i,k|k-1} - \hat{m{x}}_{k|k-1}]^T + m{Q}_k
15:
                 Update:
                  \boldsymbol{L} = [\boldsymbol{L}_1, \dots, \boldsymbol{L}_{n_x}] = \operatorname{chol}(\boldsymbol{P}_{k-1|k})
16:
                  \boldsymbol{\mathcal{X}}_{0,k|k-1} = \hat{\boldsymbol{x}}_{k|k-1}
17:
                  \mathcal{X}_{i,k|k-1} = \hat{x}_{k|k-1} + \sqrt{\lambda + n_x} L_i, i = 1, \dots, n_x
18:
                  \boldsymbol{\mathcal{X}}_{i+n_x,k|k-1} = \hat{\boldsymbol{x}}_{k|k-1} - \sqrt{\lambda + n_x} \boldsymbol{L}_i, i = 1,\dots, n_x
19:
                  \mathbf{Z}_{i,k|k-1} = \mathbf{h}(\mathbf{X}_{i,k|k-1}), i = 0, \dots, 2n_x
20:
                  \hat{\pmb{z}}_{k|k-1} = \sum_{i=0}^{2n_x} W_i^{(m)} \pmb{\mathcal{Z}}_{i,k|k-1}
21:
                  egin{align*} & P_{xz,k|k-1} = \sum_{i=0}^{2n_x} W_i^{(c)} [m{\mathcal{X}}_{i,k|k-1} - \hat{m{z}}_{k|k-1}] [m{\mathcal{Z}}_{i,k|k-1} - \hat{m{z}}_{k|k-1}]^T \ & P_{z,k|k-1} = \sum_{i=0}^{2n_x} W_i^{(c)} [m{\mathcal{Z}}_{i,k|k-1} - \hat{m{z}}_{k|k-1}] [m{\mathcal{Z}}_{i,k|k-1} - \hat{m{z}}_{k|k-1}]^T \ & S_{k|k-1} = P_{z,k|k-1} + R_k \end{split}
22:
23:
24:
                  K_k = P_{xz,k|k-1}S_{k|k-1}^{-1}
25:
                  \hat{m{x}}_{k|k} = \hat{m{x}}_{k|k-1} + m{K}_k(m{z}_k - \hat{m{z}}_{k|k-1})
26:
                 Recalibrate:
                  \mathcal{X}_{i,k|k} = \mathcal{X}_{i,k|k-1} + K_k(z_k - \hat{z}_{k|k-1}), i = 0, \dots, 2n_x
27:
                  \boldsymbol{\mathcal{Z}}_{i,k|k} = \boldsymbol{h}(\boldsymbol{\mathcal{X}}_{i,k|k}), i = 0, \dots, 2n_x
28:
                  \hat{oldsymbol{z}}_{k|k} = \sum_{i=0}^{2n_x} W_i^{(m)} oldsymbol{\mathcal{Z}}_{i,k|k}
29:
                  oldsymbol{P}_{xz,k|k} = \sum_{i=0}^{2n_x} W_i^{(c)} [oldsymbol{\mathcal{X}}_{i,k|k} - \hat{oldsymbol{x}}_{k|k}] [oldsymbol{\mathcal{Z}}_{i,k|k} - \hat{oldsymbol{z}}_{k|k}]^T
30:
                  egin{aligned} oldsymbol{P}_{z,k|k} &= \sum_{i=0}^{2n_x} W_i^{(c)} [oldsymbol{\mathcal{Z}}_{i,k|k} - \hat{oldsymbol{z}}_{k|k}] [oldsymbol{\mathcal{Z}}_{i,k|k} - \hat{oldsymbol{z}}_{k|k}]^T \ oldsymbol{S}_{k|k} &= oldsymbol{P}_{z,k|k} + oldsymbol{R}_k \end{aligned}
31:
32:
                  oldsymbol{P}_{k|k} = oldsymbol{P}_{k|k-1} + oldsymbol{K}_k oldsymbol{S}_{k|k} oldsymbol{K}_k^T - oldsymbol{P}_{xz,k|k} oldsymbol{K}_k^T - oldsymbol{K}_k oldsymbol{P}_{xz,k|k}^T
33:
                 Back out:
34:
                  if \operatorname{tr}(\boldsymbol{P}_{k|k}) > \operatorname{tr}(\boldsymbol{P}_{k|k-1}) then
35:
                           \hat{\boldsymbol{x}}_{k|k} = \hat{\boldsymbol{x}}_{k|k-1}
36:
                           P_{k|k} = P_{k|k-1}
37:
38: end for
```

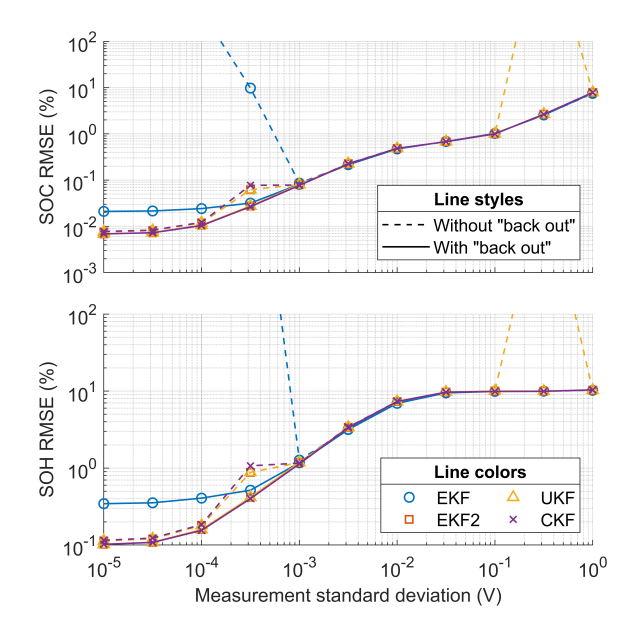


Fig. D.3. The root mean squared error of the state estimations with and without the "back out" step under different measurement noise setups (battery state estimation).

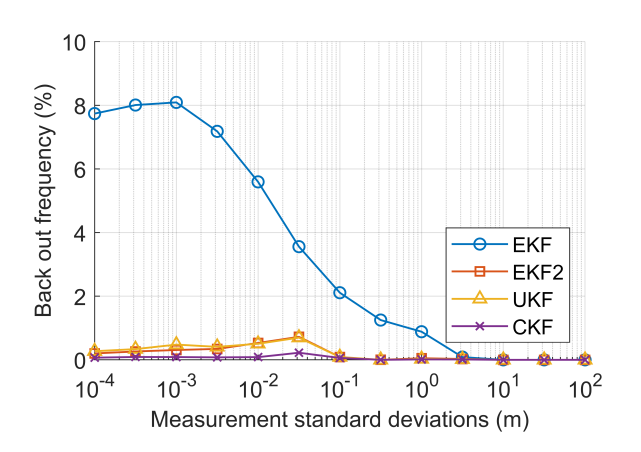


Fig. D.4. Percentage of state updates that trigger "back out" (3D target tracking).

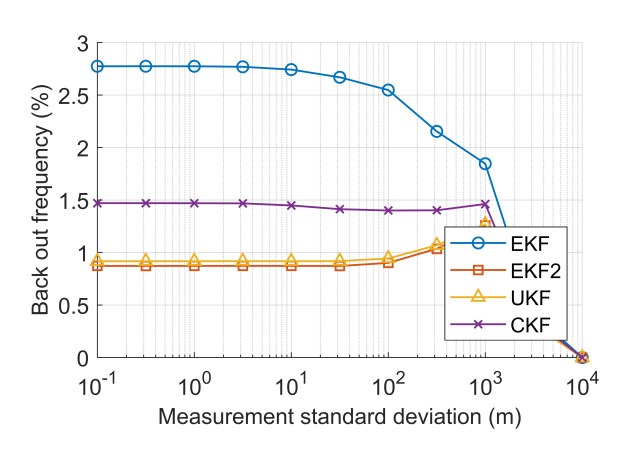


Fig. D.5. Percentage of state updates that trigger "back out" (terrain-referenced navigation).

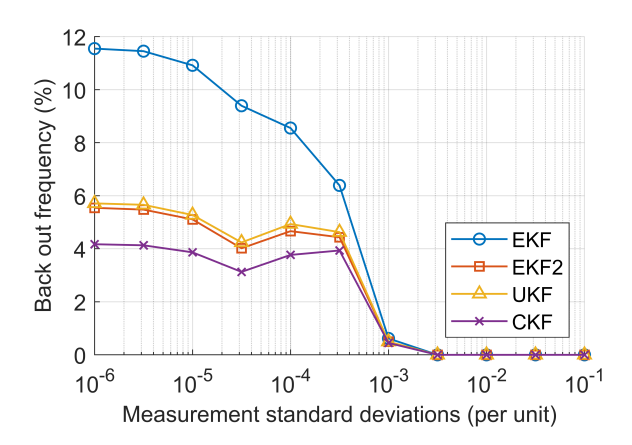


Fig. D.6. Percentage of state updates that trigger "back out" (synchronous generator state estimation).

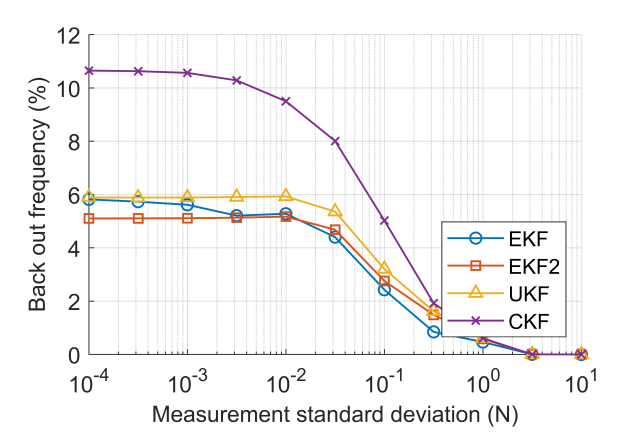


Fig. D.7. Percentage of state updates that trigger "back out" (pendulum state estimation).

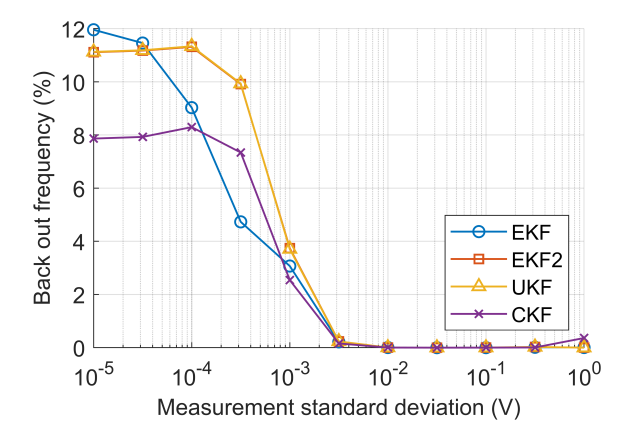


Fig. D.8. Percentage of state updates that trigger "back out" (battery state estimation).